Electronic Supplementary Material (ESI) for ChemComm.

Supporting Information

Imidazolium salts and $[Pt(cod)_2]$: from NHC hydrido complexes to the unprecedented olefinic tetrahedral cluster $[Pt_4(\mu\text{-}H)(cod)_4]BF_4$

Fengkai HE,[a,b] Christophe GOURLAOUEN,[c] Huan PANG,*[a] Pierre BRAUNSTEIN*[b]

[a] School of Chemistry and Chemical Engineering, Yangzhou University
Yangzhou, 225009, Jiangsu, P. R. China

[b] Université de Strasbourg, CNRS, Institut de Chimie UMR 7177, Institut Le Bel, 4 rue Blaise Pascal, 67081 Strasbourg Cedex, France

[c] Université de Strasbourg, CNRS, Institut de Chimie UMR 7177, Laboratoire de Chimie Quantique, 1 rue Blaise Pascal, 67081 Strasbourg Cedex, France

Table of Contents

Experimental Details 3
1. Synthesis and Characterization 3
1.1. General methods. 3
1.2. Preparation of $[Pt(cod)_2]$. 3
1.3. Preparation of $[ImH\{C(Me)=NDipp\}_2]Cl$ (1·Cl). 3
1.4. Preparation of $[Pt(H)Cl\{Im[C(Me)=NDipp]_2\}]$ (3). 3
1.5. Preparation of $[PtCl(MeO_2CC=CHCO_2Me)\{Im[C(Me)=NDipp]_2\}]$ (4). 4
1.6. Preparation of $[(ImH)\{C(Me)=NDipp\}(C_3NMe_2)]Cl$ (5·Cl). 4
1.7. Preparation of $[(ImH)\{C(Me)=NDipp\}(C_3NMe_2)]BF_4$ (5·BF_4). 4
1.8. Preparation of $[Pt(H)Cl(Im)\{C(Me)=NDipp\}(C_3NMe_2)]$ (6). 5
1.9. Preparation of $[ImH\{C(Me)=NDipp\}_2]BF_4$ (1·BF_4). 5
1.10. Preparation of $[HPt_4(C_8H_{12})_4]^+BF_4^-$ (7) 6
1.11. Other reactions 7
1.12. NMR spectra. 9
1.13. Mass spectra. 16
2. X-ray crystallography 18
2.1. General methods 18
2.2. Summary of crystal data. 19
2.3. Crystal Structure of 3 20
2.4. Crystal Structure of 4 20
2.5. Crystal Structure of 6 21
2.6. Crystal Structure of 7 22
3. Computational details 25
References 27

Experimental Details

1. Synthesis and Characterization

1.1. General methods.

All manipulations involving organometallics were performed under nitrogen or argon in a Braun glove-box or using standard Schlenk techniques. All solvents were dried using standard methods and distilled under nitrogen prior use. The starting materials $[Pt(cod)_2]$,[1] **1**·Cl,[2] **1**·BF_4[2] and **5**·Cl[3] were prepared according to the literature.

^1H, ^{13}C, ^{31}P, ^{11}B, ^{19}F and ^{195}Pt NMR spectra were recorded on Bruker spectrometers (AVANCE III – 400 MHz or AVANCE I – 500 MHz equipped with a cryogenic probe). Downfield shifts are reported in ppm as positive and referenced using signals of the residual proton solvent (^1H), the solvent (^{13}C) or externally (^{31}P). All NMR spectra were measured at 298 K, unless otherwise specified.

Mass spectra were recorded on a Bruker micrOTOF II instrument.

Elemental analyses were performed by the "Service de microanalyses", Université de Strasbourg.

1.2. Preparation of $[Pt(cod)_2]$.

This complex was prepared according to the literature.[1]

1.3. Preparation of [ImH{C(Me)=NDipp}$_2$]Cl (1·Cl).

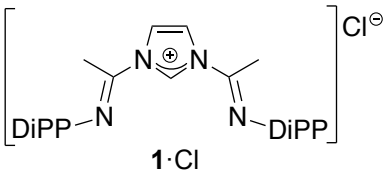

1·Cl

The bis(imine)imidazolium chloride **1**·Cl was prepared according to the literature.[2]

1.4. Preparation of [Pt(H)Cl{Im[C(Me)=NDipp]$_2$}] (3).

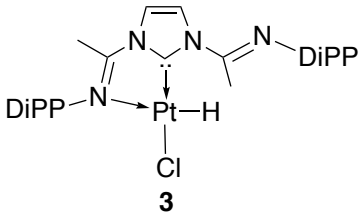

3

A mixture of **1**·Cl (100.0 mg, 0.197 mmol), $[Pt(cod)_2]$ (81.1 mg, 0.197 mmol) and pentane (20 ml) was stirred at room temperature for 12 h. The solid was collected by filtration and was dissolved in toluene. The solution was concentrated by evaporation and a yellow solid precipitated, it was collected by filtration and washed with diethyl ether. X-ray quality yellow crystals were obtained by slow diffusion of pentane into a THF solution (90.1 mg, yield 65.1%). ^1H NMR (500 MHz, C_6D_6): δ 7.34 (d, *J* = 2.5 Hz, 1H, $CH^{imidazole}$), 7.19 (s, 3H, CH^{Ar}), 7.10–7.06 (m, 3H, CH^{Ar}), 6.14 (d, *J* = 2.5 Hz, 1H, $CH^{imidazole}$), 3.19 (sept, *J* = 6.9 Hz, 2H, CH^{iPr}), 2.82 (sept, *J* = 6.9 Hz, 2H, CH^{iPr}), 2.59 (s, 3H, $CH_3{}^{imine}$), 1.51 (d,

J = 6.8 Hz, 6H, CH_3^{iPr}), 1.30 (s, 3H, CH_3^{imine}), 1.11 (d, *J* = 6.9 Hz, 6H, CH_3^{iPr}), 1.10 (d, *J* = 6.9 Hz, 6H, CH_3^{iPr}), 1.03 (d, *J* = 6.9 Hz, 6H, CH_3^{iPr}), -16.02 (s with ^{195}Pt satellites, ^1J(H-Pt) = 1530 Hz, 1H, Pt-H). ^{13}C NMR (126 MHz, C_6D_6) δ 162.37 (carbene), 158.23 (C^{imine}), 155.90 (C^{imine}), 142.79, 141.49, 138.62, 136.47, 125.41, 123.84, 123.77, 120.33, 115.08, 28.77, 28.73, 24.26, 24.04, 23.63, 22.94, 20.96, 14.52. ESI-MS: *m/z* $[C_{31}H_{43}N_4ClPt+H]^+$ $(M+1)^+$ 702.29. Anal. calcd. for $C_{31}H_{43}N_4ClPt$: C, 53.02; H, 6.17; N, 7.98%; found: C, 52.34; H, 6.22; N, 7.87%.

1.5. Preparation of [PtCl(MeO$_2$CC=CHCO$_2$Me){Im[C(Me)=NDipp]$_2$}] (4).

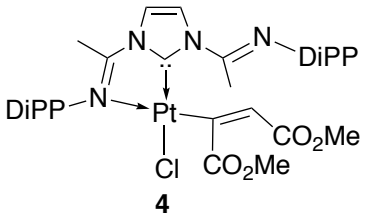

4

A mixture of **3** (50.0 mg, 0.0712 mmol), dimethylacetylenedicarboxylate (12.2 mg, 0.0854 mmol) and toluene (10 ml) was stirred at room temperature for 1 h. The solution was concentrated, and diethyl ether (10 ml) was added. The pure yellow solid precipitated and was obtained in 92.8% yield. X-ray quality yellow crystals were obtained from a saturated benzene solution. ^{1}H NMR (400 MHz, CD_2Cl_2): δ 7.63 (d, *J* = 2.3 Hz, 1H, $CH^{imidazole}$), 7.47 (d, *J* = 2.3 Hz, 1H, $CH^{imidazole}$), 7.38 – 7.14 (m, 6H, CH^{Ar}), 4.95 (s with ^{195}Pt satellites, ^3J(H-Pt) = 40 Hz, 1H, C=CH), 3.45 (s, 3H, OMe), 3.40 (s, 3H, OMe), 3.04 (sept, *J* = 6.9 Hz, 4H, CH^{iPr}), 2.63 (s, 3H, CH_3^{imine}), 2.17 (s, 3H, CH_3^{imine}), 1.31 (d, *J* = 6.9 Hz, 6H, CH_3^{iPr}), 1.28 (d, *J* = 6.9 Hz, 6H, CH_3^{iPr}), 1.17 (d, *J* = 6.9 Hz, 6H, CH_3^{iPr}), 1.11 (d, *J* = 6.9 Hz, 6H, CH_3^{iPr}). ^{13}C NMR (126 MHz, CD_2Cl_2, assignments from HMQC and HMBC): δ 178.68 (carbene), 176.07 (C=O), 169.61 (C=O), 164.93 (C-Pt), 164.89 (coordinated C^{imine}), 156.6 (dangling C^{imine}), 142.38, 142.26, 139.93, 136.95, 129.13, 125.36, 124.52, 124.29, 124.20, 123.74 (CH^{imid}), 116.85 (CH^{imid}), 50.86, 50.78, 28.51, 28.45, 24.44, 23.84, 23.40, 23.01, 22.49, 17.65. ESI-MS: *m/z* $[C_{37}H_{49}ClN_4O_4Pt+Na]^+$ 866.30. Anal. calcd. for $C_{37}H_{49}ClN_4O_4Pt$: C, 52.63; H, 5.85; N, 6.64%; found: C, 51.71; H, 5.87; N, 6.51%.

1.6. Preparation of [(ImH){C(Me)=NDipp}(C$_3$NMe$_2$)]Cl (5·Cl).

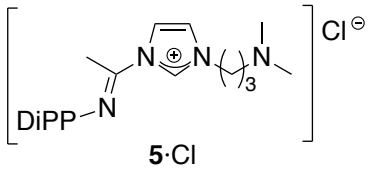

5·Cl

The amine, imine imidazolium chloride **5**·Cl was prepared according to the literature.[3]

1.7. Preparation of [(ImH){C(Me)=NDipp}(C$_3$NMe$_2$)]BF$_4$ (5·BF$_4$).

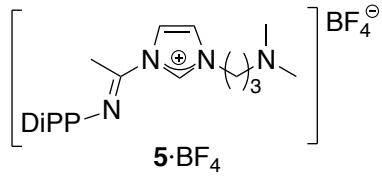

5·BF_4

A mixture of **5**·Cl (1.00 g, 2.56 mmol) and $AgBF_4$ (497.9 mg, 2.56 mmol) in THF (20 ml) was stirred for 1 h at room temperature and a white precipitate of AgCl formed. Filtration through a Celite pad

afforded a transparent solution which was evaporated under reduced pressure. The residue was dissolved in toluene, the solution was filtered through Celite and concentrated under reduced pressure, affording white needles of the product (1.10 g, yield 97.2%). ^{1}H NMR (400 MHz, $CDCl_3$): δ 9.60 (br s, 1H, CH^{imid}), 8.17 (br s, 1H, CH^{imid}), 7.60 (dd, *J* = 2.8, 2.3 Hz, 1H, CH^{imid}), 7.16 (br s, 3H, CH^{Ar}), 4.51 (t, *J* = 6.9 Hz, 2H, $\underline{CH_2}CH_2CH_2NMe_2$), 2.64 (sept, *J* = 6.9 Hz, 2H, CH^{iPr}), 2.51 (t, *J* = 6.7 Hz, 2H, $CH_2CH_2\underline{CH_2}NMe_2$), 2.39 (s, 3H, CH_3^{imine}), 2.31 (s, 6H, $CH_2CH_2CH_2N\underline{Me_2}$), 2.20 (apparent q, ^{3}J = 6.7 Hz, 2H, $CH_2\underline{CH_2}CH_2NMe_2$), 1.15 (d, *J* = 6.9 Hz, 6H, CH_3^{iPr}), 1.11 (d, *J* = 6.9 Hz, 6H, CH_3^{iPr}). ^{13}C NMR (126 MHz, $CDCl_3$): δ 148.52 (C^{imid}), 140.77, 136.77, 136.33, 125.62, 123.63, 123.57, 118.12, 55.06, 48.60, 44.91, 28.55, 27.04, 23.36, 22.96, 15.82. ESI-MS: *m/z* $[C_{22}H_{35}N_4]^+$ 355.29. Anal. calcd. for $C_{22}H_{35}BF_4N_4$: C, 59.74; H, 7.98; N, 12.67%; found: C, 58.28; H, 7.87; N, 12.38%.

1.8. Preparation of [Pt(H)Cl(Im){C(Me)=NDipp}(C_3NMe_2)] (6).

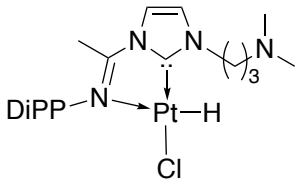

6

A mixture of **5**·Cl (100.0 mg, 0.256 mmol) and $[Pt(cod)_2]$ (105.2 mg, 0.256 mmol) in THF (20 ml) was stirred at room temperature for 24 h. The solvent was removed under vacuum, the residue was extracted with toluene to give a green yellow solution that was concentrated, affording a yellow solid. X-ray quality yellow crystals were obtained by slow diffusion of pentane into a THF solution (60.0 mg, yield 40%). ^{1}H NMR (400 MHz, THF-d_8): δ 7.59 (d, *J* = 2.0 Hz, 1H, CH^{imid}), 7.22 (d, *J* = 2.0 Hz, 1H, CH^{imid}), 7.24–7.16 (m, 3H, $CH^{p\text{-}Ar}$, $CH^{m\text{-}Ar}$), 4.14 (t, *J* = 7.1 Hz, 2H, $\underline{CH_2}CH_2CH_2NMe_2$), 3.03 (sept, *J* = 6.5 Hz, 2H, CH^{iPr}), 2.32 (t, *J* = 6.4 Hz, 2H, $CH_2CH_2\underline{CH_2}NMe_2$), 2.21 (s, 6H, $CH_2CH_2CH_2N\underline{Me_2}$), 2.15 (s, 3H, CH_3^{imine}), 2.05 (apparent q, *J* = 6.7 Hz, 2H, $CH_2\underline{CH_2}CH_2NMe_2$), 1.25 (d, *J* = 6.7 Hz, 6H, CH_3^{iPr}), 1.10 (d, *J* = 6.9 Hz, 6H, CH_3^{iPr}), -17.37 (s with ^{195}Pt satellites, *J* = 1568 Hz, 1H, Pt-H). ^{13}C NMR (126 MHz, THF-d_8): δ 164.39, 160.35, 141.93, 139.74, 127.23, 123.52, 122.16, 116.50, 56.58, 51.05, 45.43, 28.62, 28.49, 24.19, 23.90, 14.65. ESI-MS: *m/z* $[C_{22}H_{35}ClN_4Pt+H]^+$ $(M+H)^+$ 586.23. Anal. calcd. for $C_{22}H_{35}ClN_4Pt$: C, 45.09; H, 6.02; N, 9.56%; found: C, 44.65; H, 6.03; N, 9.33%.

1.9. Preparation of [ImH{C(Me)=NDipp}$_2$]BF_4 (1·BF_4).

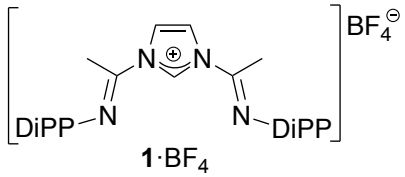

1·BF_4

The bis(imine)imidazolium tetrafluoroborate **1**·BF_4 was prepared according to the literature.[2]

1.10. Preparation of $[HPt_4(C_8H_{12})_4]^+BF_4^-$ (7).

A mixture of **1**·BF_4 (50 mg, 0.0895 mmol), [Pt(cod)$_2$] (147.3 mg, 0.358 mmol) and THF (10 ml) was stirred at room temperature overnight and a dark red solid precipitated. This pure solid was collected by filtration (20 mg, 0.0154 mmol, 17.2%). X-ray quality crystals were obtained from CH_2Cl_2/pentane solution. ^{1}H NMR (400 MHz, CD_2Cl_2): δ 5.05 (br s, 16H, =CH), 2.20 (br s, 16H, CH_2), 1.97 (m, 16H, CH_2), -6.87 (sept, *J* = 350 Hz, 1H, Pt-H, see below and Figure S1). ^{13}C NMR (126 MHz, CD_2Cl_2): δ 95.58, 92.99, 30.74. ^{11}B NMR (96 MHz, CD_2Cl_2) δ -1.16. ^{19}F NMR (282 MHz, CD_2Cl_2) δ -153.46 ($^{10}BF_4$), -153.52 ($^{11}BF_4$). ^{195}Pt{^{1}H} NMR (107 MHz, CD_2Cl_2): δ 2863 (s). ^{195}Pt NMR (107 MHz, CD_2Cl_2): δ 2863 (d, *J* = 350 Hz). ESI-MS: *m/z* $[Pt_4(C_8H_{12})_4H]^+$ (M^+) 1213.24 (100%), $[Pt_4(C_8H_{12})_3]^+$ (*M*-cod$^+$) 1104.14 (31%). Anal. calcd. for $[PtC_8H_{12}]_4HBF_4$: C, 29.55; H, 3.80%; found: C, 28.32; H, 3.70%.

Simulation of the ^{1}H NMR hydride resonance (Figure S1). This signal has the appearance of a septet resulting from the superposition of five subspectra corresponding to the isotopomers containing 0-4 ^{195}Pt (*S* =1/2, natural abundance 33.8%):

Isotopomer with zero ^{195}Pt: probability: 0.662 x 0.662 x 0.662 x 0662 x 1 = 19.21% (singlet)

Isotopomer with one ^{195}Pt: probability: 0.662 x 0.662 x 0.662 x 0.338 x 4 = 39.22% (doublet 19.61/19.61)

Isotopomer with two ^{195}Pt: probability: 0.662 x 0.662 x 0.338 x 0.338 x 6 = 30.04% (triplet 7.51/15.02/7.51)

Isotopomer with three ^{195}Pt: probability: 0.662 x 0.338 x 0.338 x 0.338 x 4 = 10.22 (quartet 1.27/3.83/3.83/1.27)

Isotopomer with four ^{195}Pt: probability: 0.338 x 0.338 x 0.338 x 0.338 x 1 = 1.30% (quintet 0.081/0.326/0.489/0.326/0.081)

Considering that the external lines of the quintet due to the isotopomer with 4 ^{195}Pt nuclei are too weak to be observed, the relative integrations of the 7 peaks A-G (Figure S1) should therefore be as follows:

A: 1.27

B: 7.51 + 0.33 = 7.84

C: 19.61 + 3.83 = 23.44

D: 19.21 + 15.02 + 0.49 = 34.72

E: 19.61 + 3.83 = 23.44

F: 7.51 + 0.33 = 7.84

G: 1.27

By setting the integration of the central peak at 34.72, there is very good agreement between the experimental and calculated values: 0.92/6.86/22.88/34.72/22.88/6.86/0.92, and 1.27/7.84/23.44/34.72/23.44/7.84/1.27, respectively.

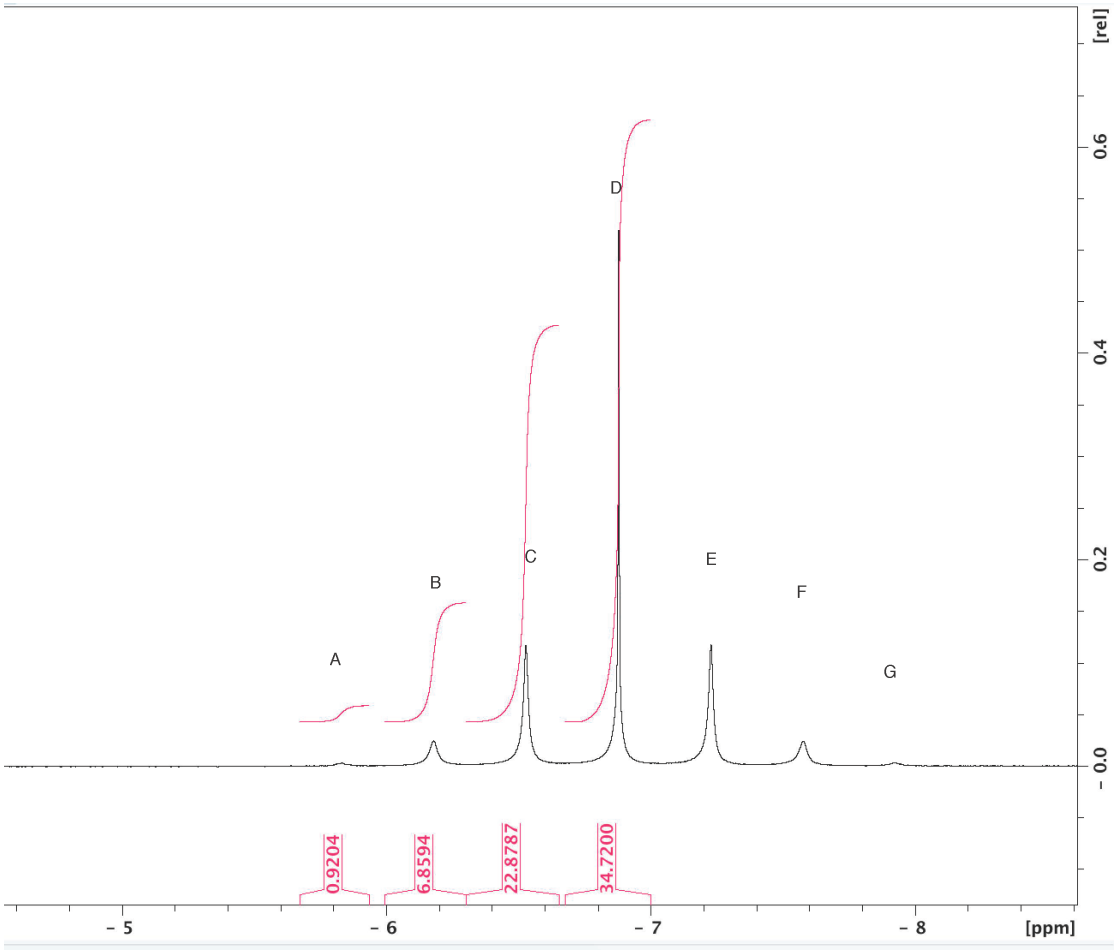

Figure S1. ^{1}H NMR spectrum of **7** in the hydride region.

1.11. Other reactions.

Reaction of 5·BF_4 with [Pt(cod)$_2$].

A mixture of **5**·BF_4 (50 mg, 113.03 μmol) and [Pt(cod)$_2$] (186.03 mg, 452.13 μmol) in THF (10 ml) was stirred for 24 h at room temperature. All volatiles were removed under vacuum and the ^{1}H

NMR spectrum the crude mixture indicated that most of the starting materials were unreacted. Traces of cluster **7** were observed, together with another Pt-hydride complex (^{1}H NMR Figure S15). However, the latter was formed in very small amount and could not be isolated.

Reaction of cluster 7 with H_2.

In a Young's tube, cluster **7** (3.84 μmol, 5.0 mg) was dissolved in CD_2Cl_2, hydrogen gas (1 atm) was introduced into the tube. The colour of the dark red solution faded away and platinum black precipitated.

Reaction of cluster 7 with ethylene.

In a Young's tube, cluster **7** (3.84 μmol, 5.0 mg) was dissolved in CD_2Cl_2, ethylene gas (1 atm) was introduced into the tube. ^{1}H NMR spectroscopy was used to monitor the reaction. The result indicated that cluster **7** remained unreacted.

Reaction of cluster 7 with CN^{t}Bu.

In a Young's tube, cluster **7** (3.84 μmol, 5.0 mg) was dissolved in CD_2Cl_2 and excess CN^{t}Bu was added. The dark red solution turned into dark yellow solution, which revealed by ^{1}H NMR the presence of free cod and the absence of a Pt-H resonance.

Reaction of cluster 7 with DMAD.

In a Young's tube, cluster **7** (3.84 μmol, 5.0 mg) was dissolved in CD_2Cl_2 and excess DMAD was added. The colour of the solution turned from dark red to orange. Free cod was observed, and a new Pt-H resonance was observed at δ -7.48 (*J*(Pt-H) = 312 Hz) but this complex could not be crystallized.

Reaction of cluster 7 with HBF_4.

In a Young's tube, cluster **7** (3.84 μmol, 5.0 mg) was dissolved in CD_2Cl_2 and one drop of 1 M HBF_4 in Et_2O was added to the solution and no colour change was observed. ^{1}H NMR monitoring indicated that the Pt-H resonance of **7** was slightly shifted (from δ -6.87 to -9.01) but its pattern remained unchanged (*J*(Pt-H) = 340 Hz).

Reaction of cluster 7 with NEt_3.

In a Young's tube, cluster **7** (3.84 μmol, 5.0 mg) was dissolved in CD_2Cl_2 and one drop of pure NEt_3 (excess) was added to the solution. ^{1}H NMR monitoring indicated that no reaction occurred.

Reaction of cluster 7 with DBU.

In a Young's tube, cluster **7** (3.84 μmol, 5.0 mg) was dissolved in C_6D_6 and one drop DBU (excess) was added. The solution became yellow and a dark precipitate formed. The ^{1}H NMR spectrum was

complicated and revealed the disappearence of the hydride resonance. The mass spectrum of the solution revealed a peak at *m/z* 1148.51, corresponding to $[Pt_4(cod)_2(DBU)]^+$.

Reaction of cluster 7 with NaH.

In a Young's tube, cluster **7** (3.84 μmol, 5.0 mg) was dissolved in THF/C_6D_6 and 1.0 mg (excess) NaH was added. The solution became yellow and a dark precipitate formed. The ^{1}H NMR spectrum was complicated and revealed the disappearence of the hydride resonance.

Reaction of cluster 7 with KHMDS.

In a Young's tube, cluster **7** (3.84 μmol, 5.0 mg) was dissolved in C_6D_6 and 1.0 mg (excess) KHMDS was added. The solution became yellow and a dark precipitate formed. The ^{1}H NMR spectrum was complicated and revealed the disappearence of the hydride resonance.

Preparation of $[HPt_4(C_8H_{12})_4]^+BF_4^-$ (7) in THF-d_8. A mixture of **1**·BF_4 (25 mg, 0.0447 mmol), $[Pt(cod)_2]$ (73.7 mg, 0.179 mmol) and THF-d_8 (4 mL) was stirred at room temperature overnight and a dark red solid precipitated. This pure solid was collected by filtration (9.5 mg, 0.0073 μmol, 16.3%). Its ^{1}H NMR spectrum confirmed the presence of the μ-H hydrido ligand.

1.12. NMR spectra.

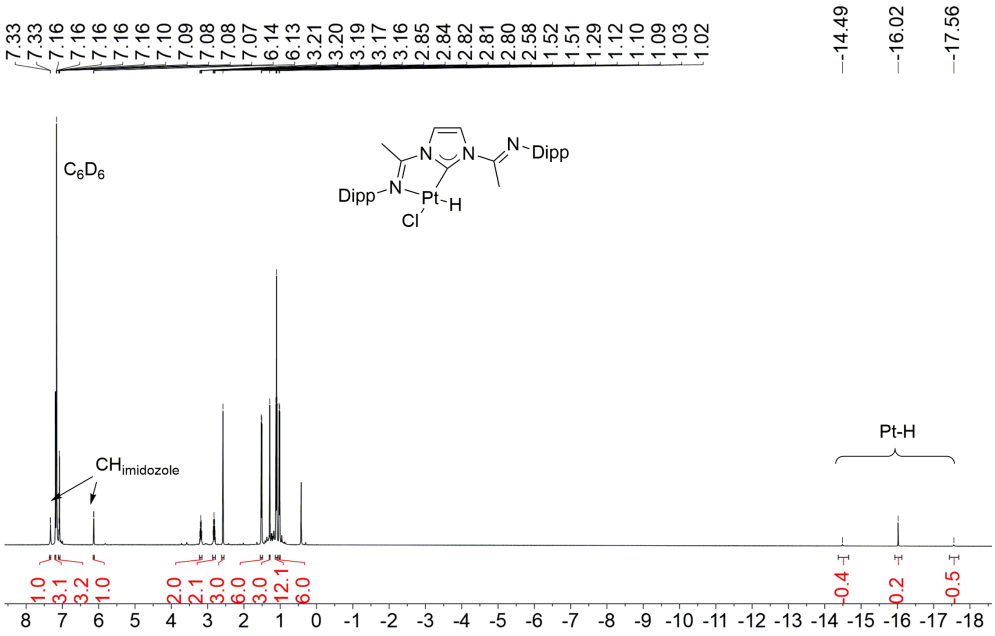

Figure S2. ^{1}H NMR spectrum of **3** in C_6D_6.

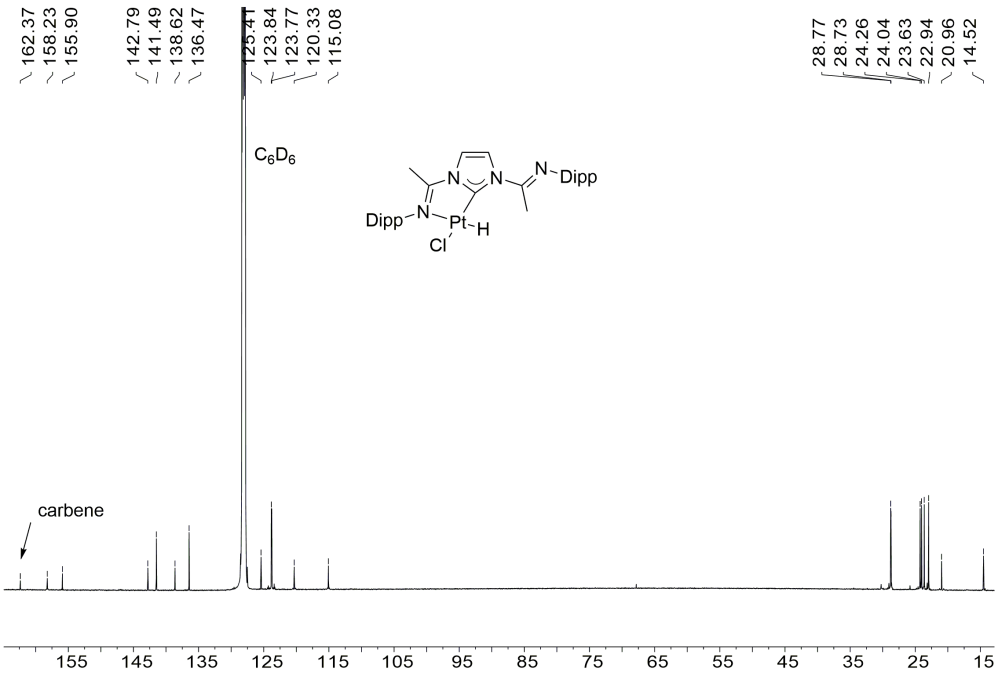

Figure S3. ^{13}C NMR spectrum of **3** in C_6D_6.

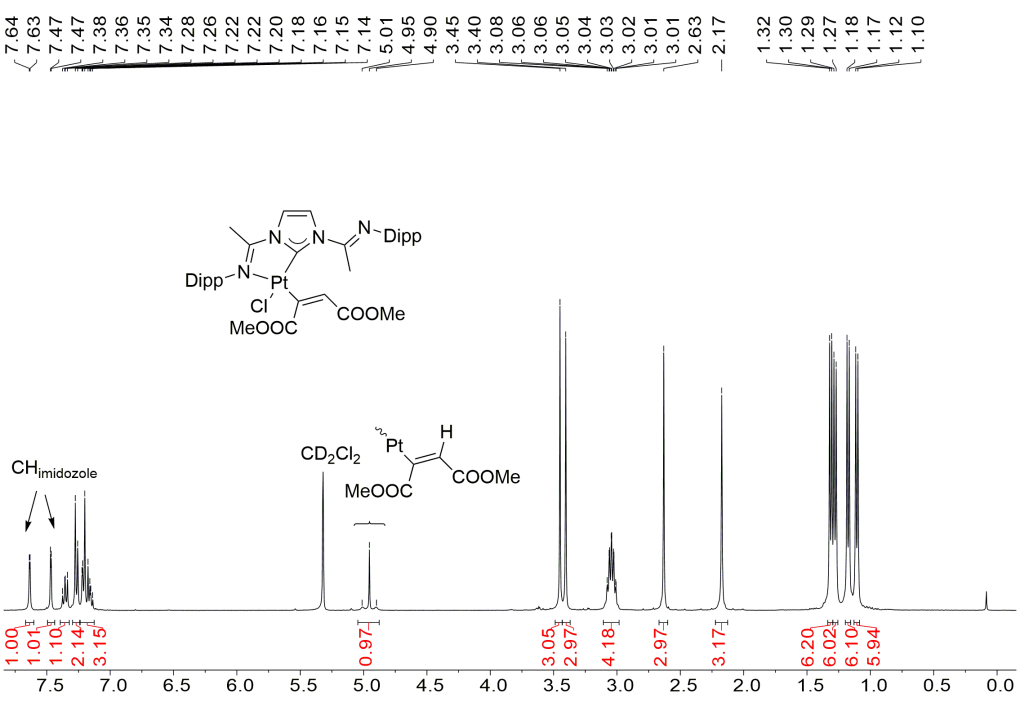

Figure S4. ^{1}H NMR spectrum of **4** in CD_2Cl_2.

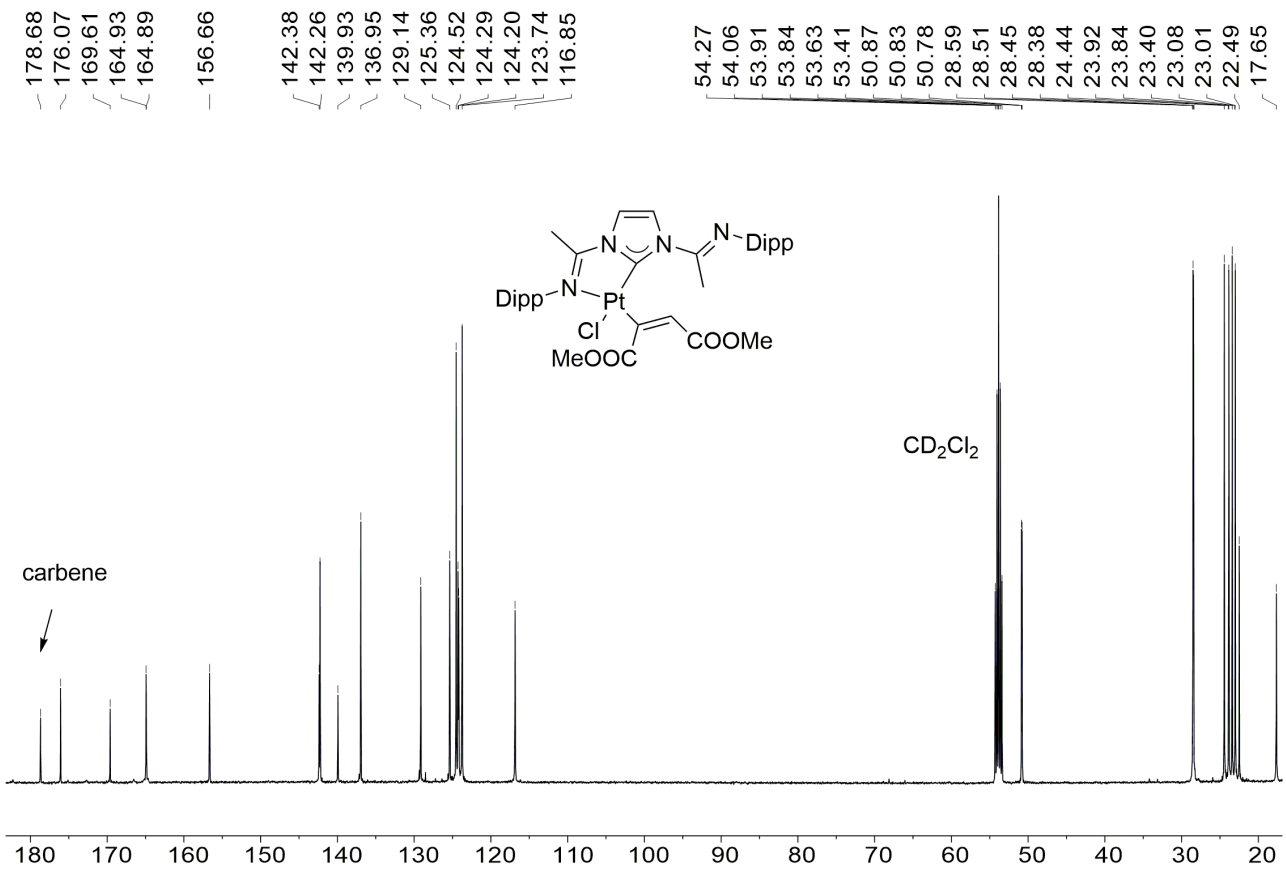

Figure S5. ^{13}C NMR spectrum of **4** in CD_2Cl_2.

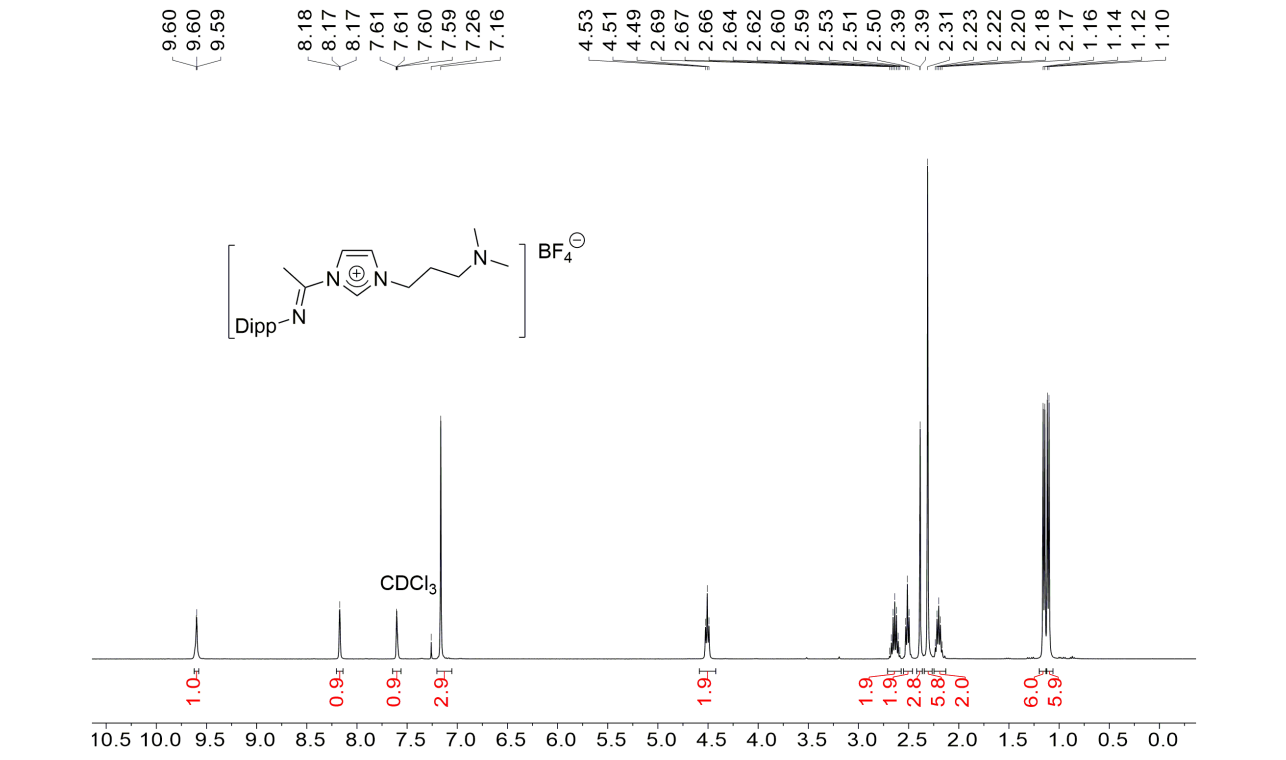

Figure S6. ^{1}H NMR spectrum of **5**·BF_4 in $CDCl_3$.

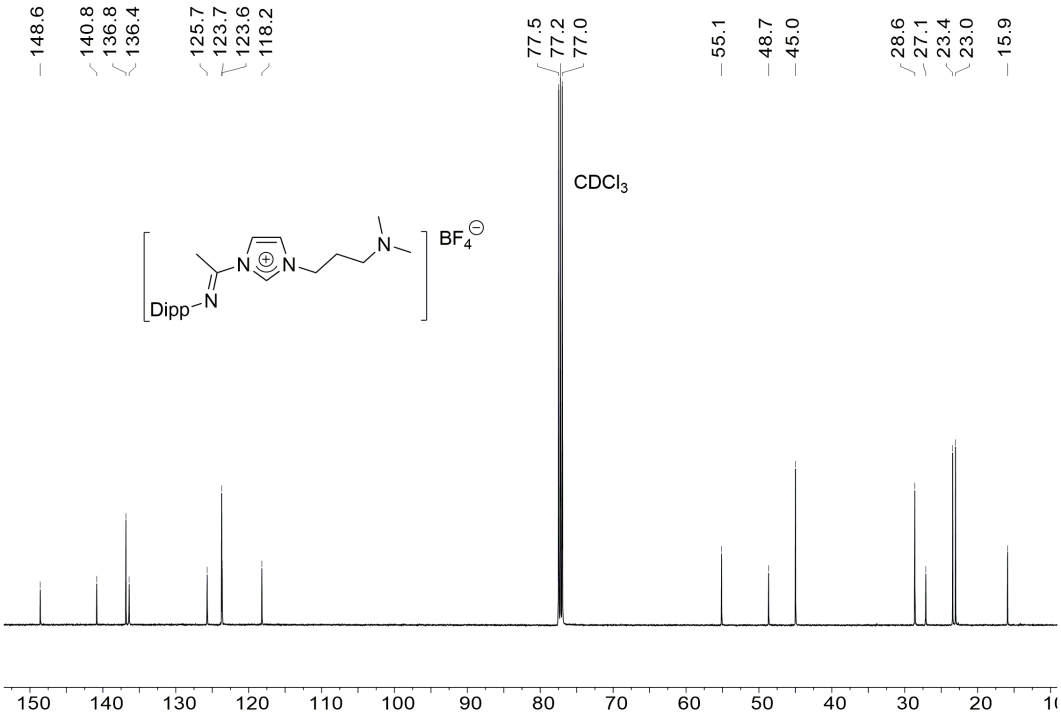

Figure S7. ^{13}C NMR spectrum of **5**·BF_4 in $CDCl_3$.

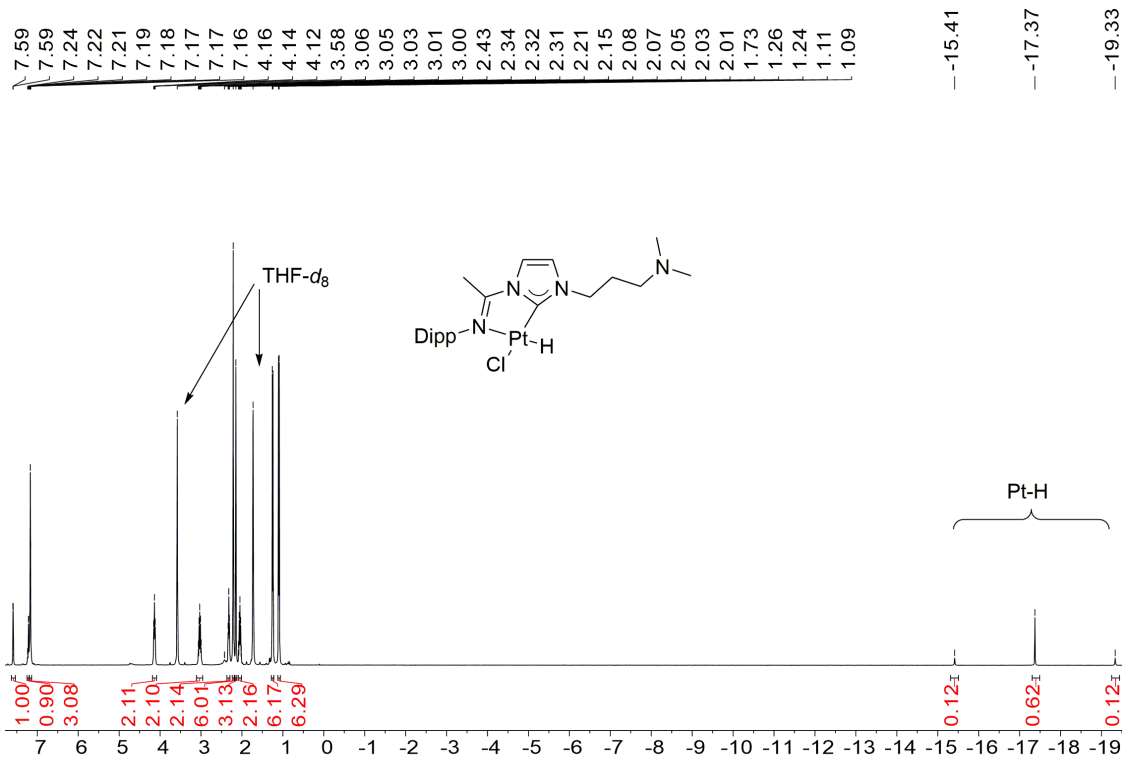

Figure S8. ^{1}H NMR spectrum of **6** in THF-d_8.

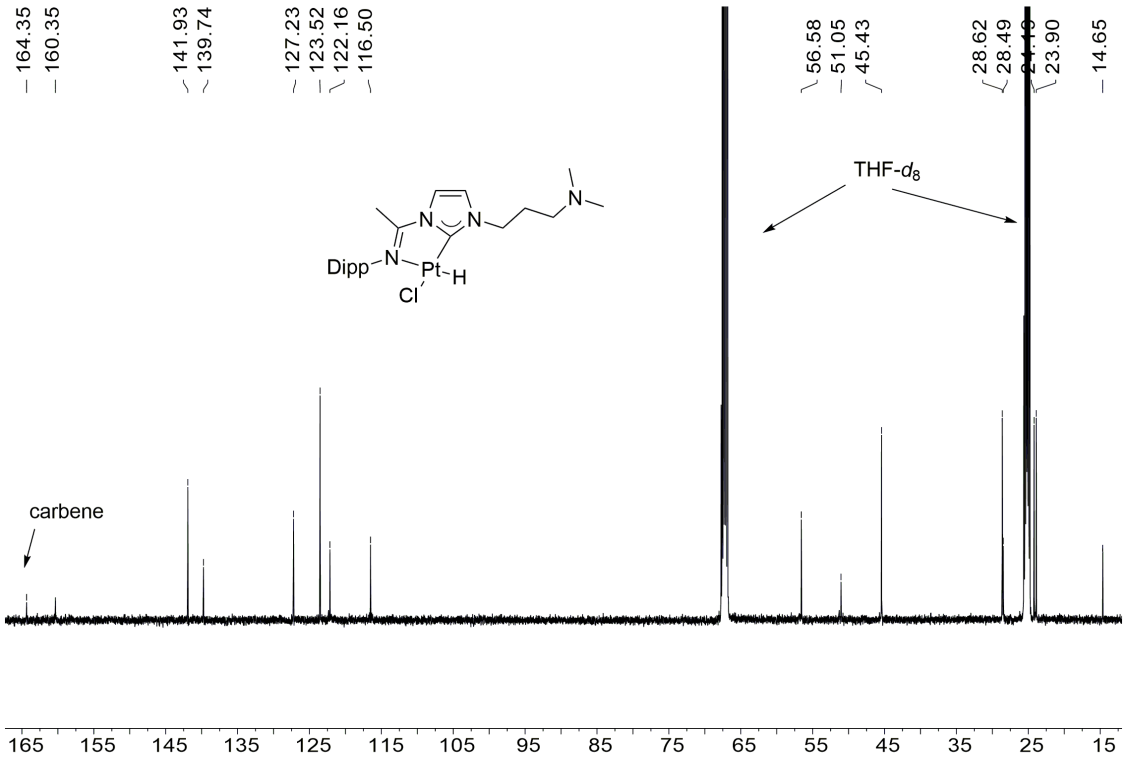

Figure S9. ^{13}C NMR spectrum of **6** in THF-d_8.

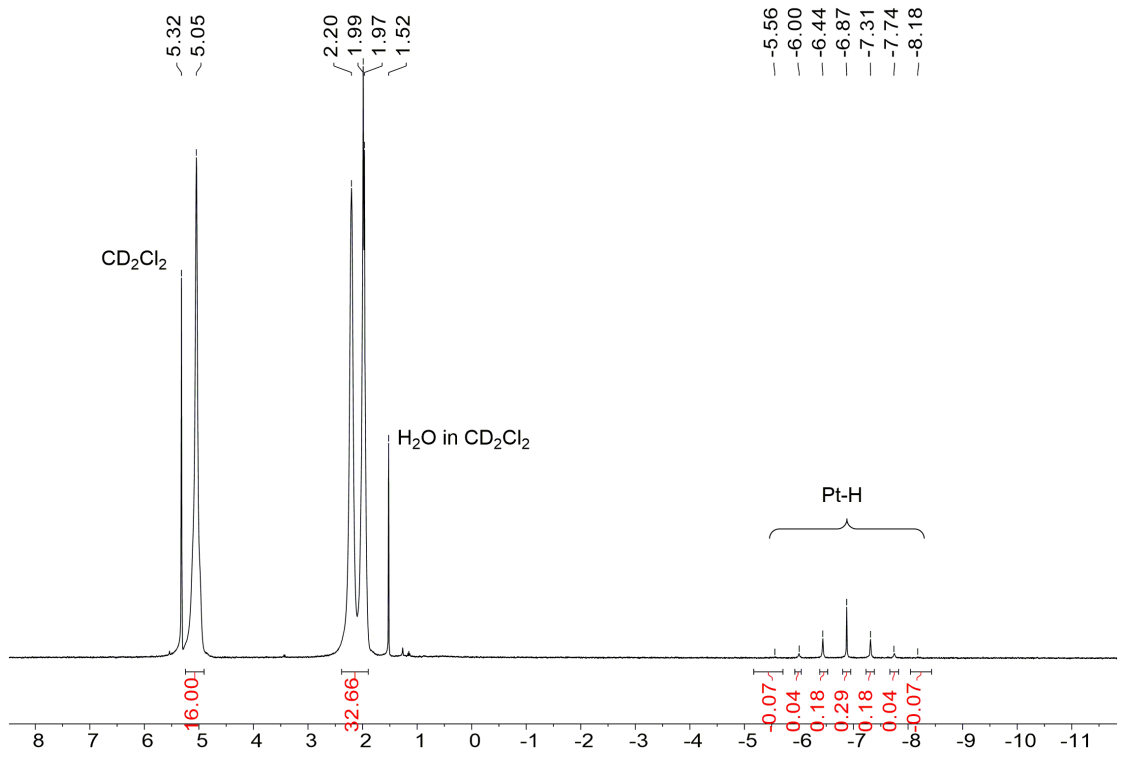

Figure S10. ^{1}H NMR spectrum of **7** in CD_2Cl_2.

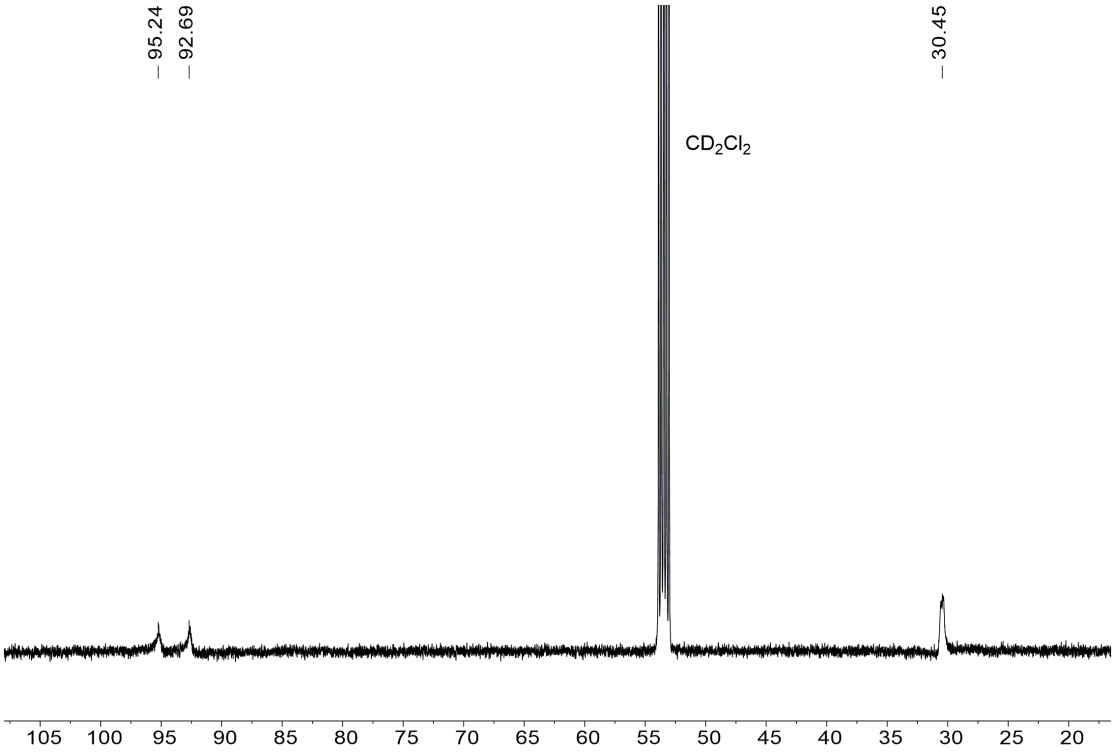

Figure S11. ^{13}C NMR spectrum of **7** in CD_2Cl_2.

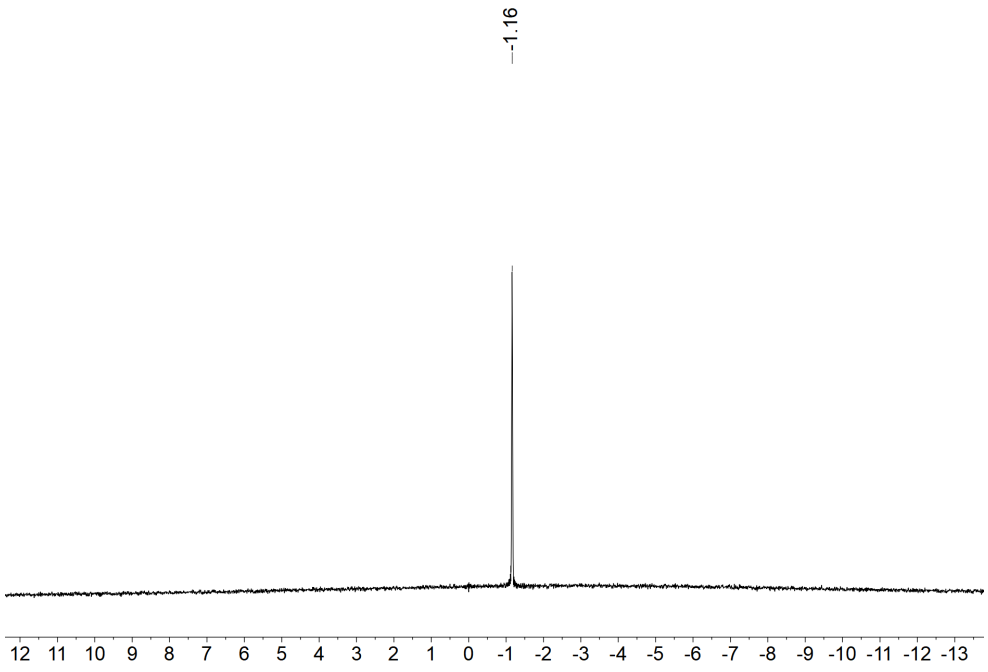

Figure S12. ^{11}B NMR spectrum of **7** in CD_2Cl_2.

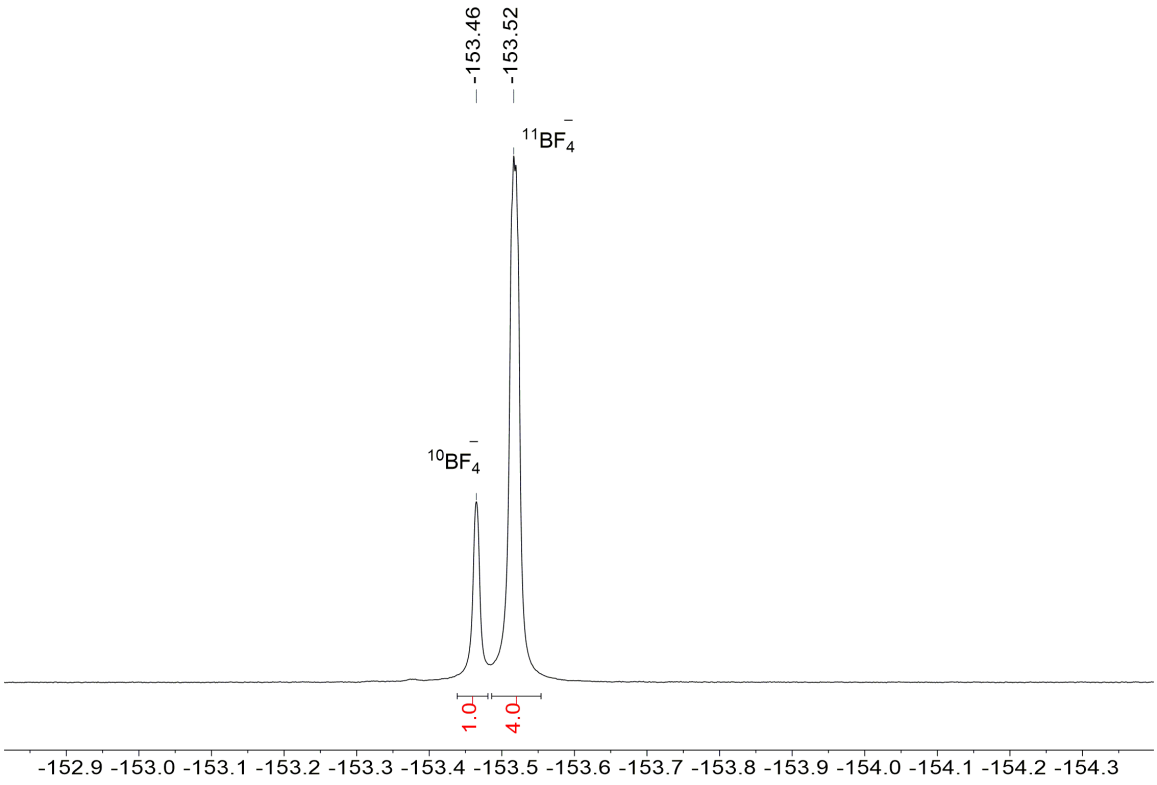

Figure S13. ^{19}F NMR spectrum of **7** in CD_2Cl_2.

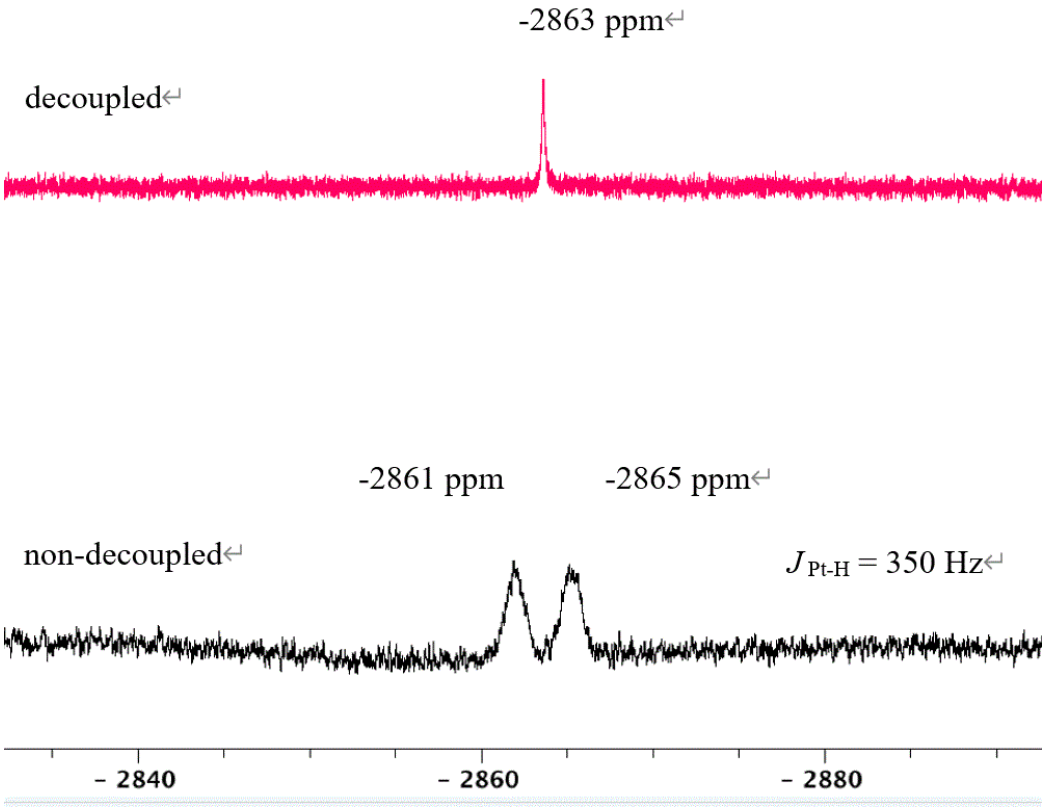

Figure S14. ^{195}Pt NMR spectrum of **7** in CD_2Cl_2.

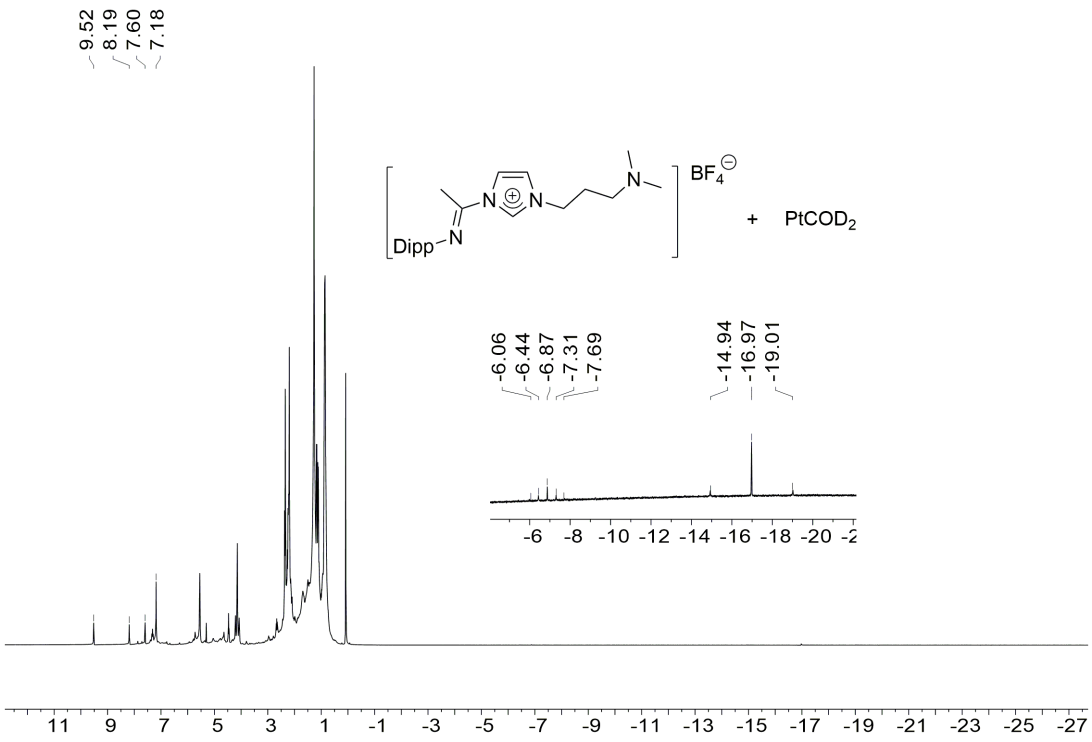

Figure S15. ^{1}H NMR spectrum of crude product in CD_2Cl_2.

1.13. Mass spectra.

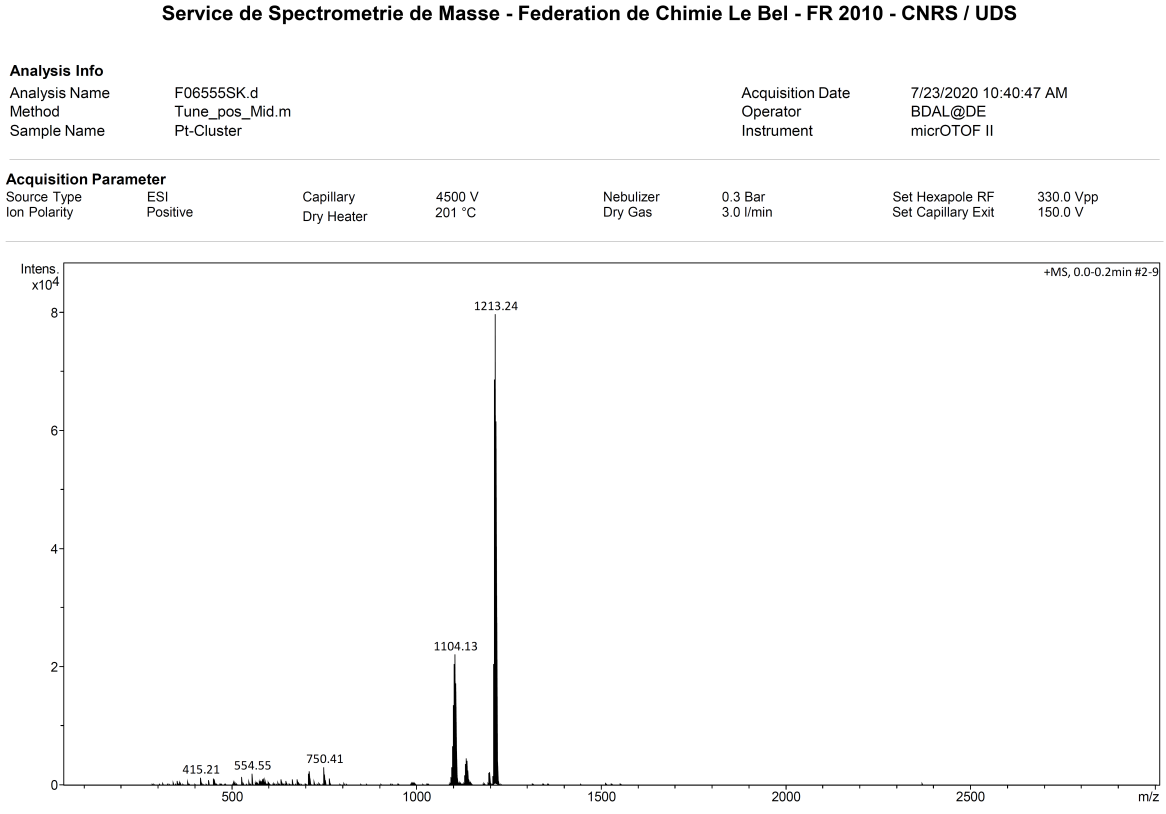

Figure S16. Full mass spectrum of **7**.

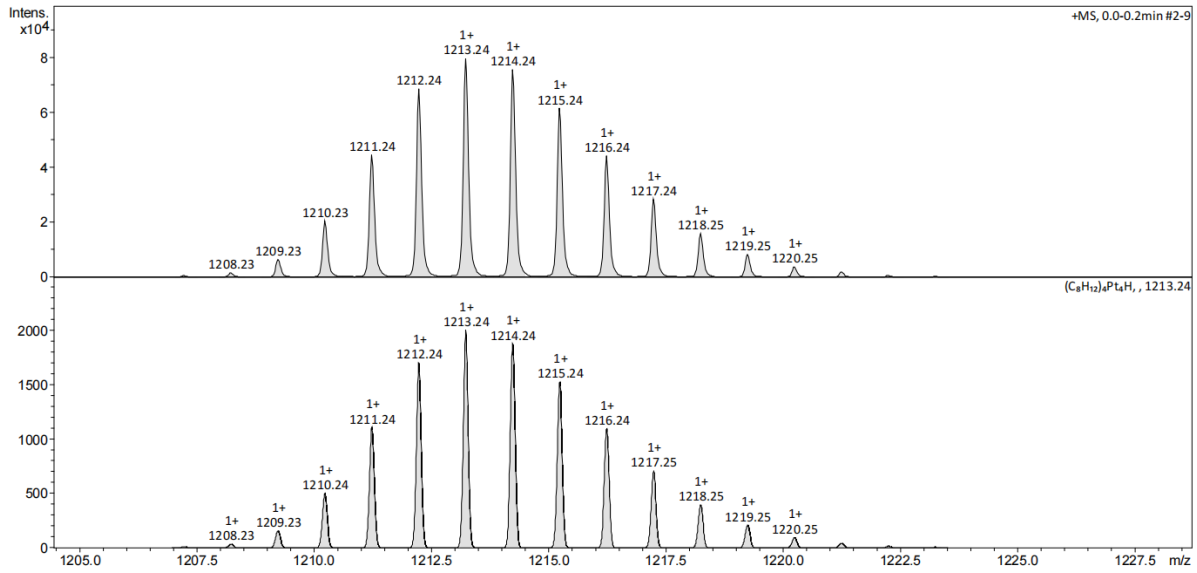

Figure S17. Partial mass spectrum and simulation of **7**.

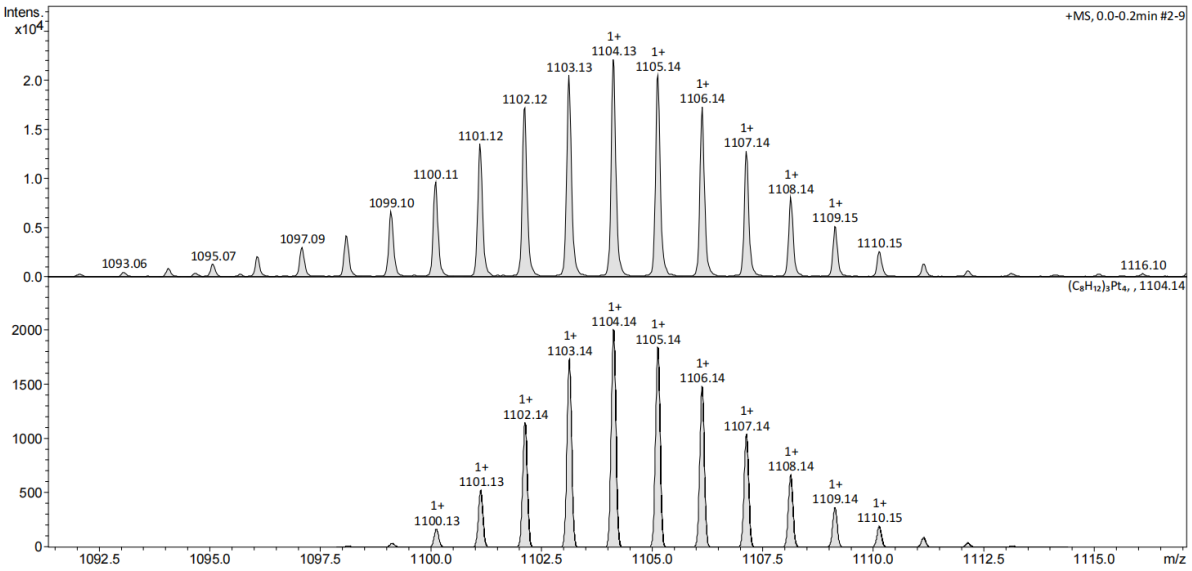

Figure S18. Partial mass spectrum and simulation of **7**.

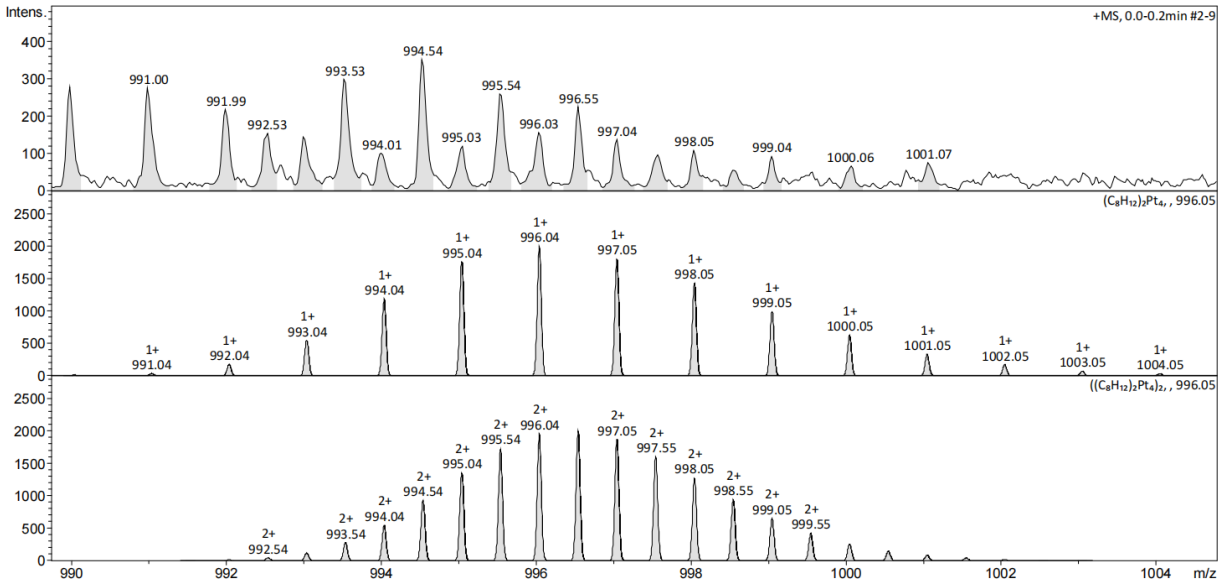

Figure S19. Partial mass spectrum and simulation of **7**.

2. X-ray crystallography

2.1. General methods

For complexes **3**, **4**·2C_6H_5 and **6**, the crystals were mounted on a glass fiber with grease, from Fomblin vacuum oil. Data sets were collected on a Bruker APEX II DUO diffractometer equipped with an Oxford Cryosystem liquid N_2 device, using Mo-Kα radiation (λ = 0.71073 Å). The crystal-detector distance was 38 mm. The cell parameters were determined (APEX2 software) from reflections taken from three sets of 12 frames, each at 10 s exposure. The structures were solved by direct methods using the program SHELXS-97.[4] The refinement and all further calculations were carried out using SHELXL-97.[5] The H-atoms were included in calculated positions and treated as riding atoms using SHELXL default parameters. The non-H atoms were refined anisotropically, using weighted full-matrix least-squares on F^2.

For **7**, the structure was solved and refined using the Bruker SHELXTL Software Package, using the space group *C*1 2/c 1, with Z = 4 for the formula unit, $C_{32}H_{51}BF_4Pt_4$. The X-ray intensity data were measured (λ = 0.71073 Å).

2.2. Summary of the crystal data.

Summary of the crystal data, data collection and refinement for the structures of **3**, **4**·$2C_6H_5$, **6** and **7** are given in Table S1.

Table S1. Crystal data for compounds **3**, **4**·$2C_6H_5$, **6** and **7**.

	3	**4**·$2C_6H_5$	**6**	**7**
Chemical formula	$C_{31}H_{43}ClN_4Pt$	$C_{37}H_{49}ClN_4O_4Pt$, $2C_6H_6$	$C_{22}H_{35}ClN_4Pt$	$C_{32}H_{49}BF_4Pt_4$
CCDC Number	2093082	2093083	2093084	2093085
Formula Mass	702.23	1000.55	586.08	-
Crystal system	orthorhombic	monoclinic	monoclinic	monoclinic
a/Å	14.9375(5)	64.377(3)	14.6958(8)	21.3229(16)
b/Å	12.7705(4)	9.8222(4)	13.8722(7)	12.7436(12)
c/Å	31.6136(10)	14.9522(5)	12.7246(6)	15.3117(14)
α/°	90	90	90	90
β/°	90	101.6410(10)	112.646(2)	132.571(3)
γ/°	90	90	90	90
Unit cell volume/Å^3	6030.6(3)	9260.1(6)	2394.1(2)	3064.1(5)
Temperature/K	120(2)	120(2)	120(2)	173(2)
Space group	*P b c a*	*C 2/c*	*P 2$_1$/c*	*C 2/c*
Formula units/cell, *Z*	8	8	4	4
Absorption coeff., *μ*/mm^{-1}	4.768	3.135	5.987	18.252
No. of reflections measured	155022	190214	77110	19035
No. of independent reflections	10516	13561	7659	4407
R_{int}	0.0547	0.0453	0.0458	0.0938
Final R_1 values ($I > 2\sigma(I)$)	0.0332	0.0196	0.0204	0.0637
Final $wR(F^2)$ values ($I > 2\sigma(I)$)	0.0701	0.0379	0.0358	0.1554
Final R_1 values (all data)	0.0537	0.0244	0.0276	0.0908
Final $wR(F^2)$ values (all data)	0.0796	0.0400	0.0386	0.1711
Goodness of fit on F^2	1.070	1.070	1.069	1.030

2.3. Crystal Structure of 3.

A chloride ligand is coordinated to the Pt atom, and one nitrogen atom of the ligand (N4) is not coordinated to the metal. One methyl group (C27) is disordered over two positions with a ratio of 0.7/0.3. The hydrogen atom H26 is also disordered. The hydride H1 was found and refined. The distance Pt1–H1 is 1.49 Å. The refinement of the structure yielded R1 = 3.3%.

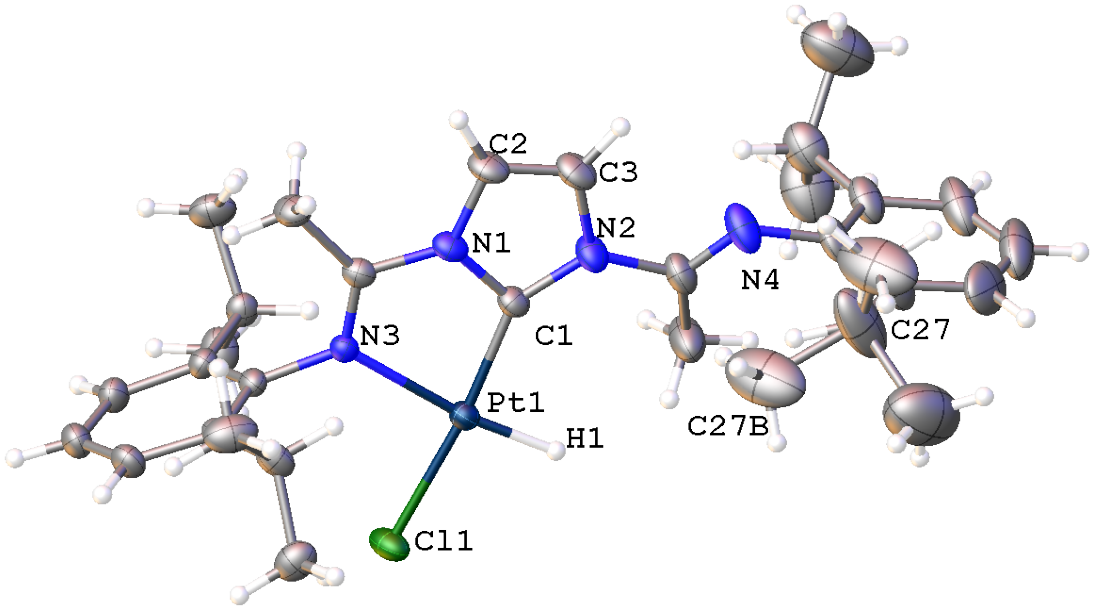

Figure S20. Structure of **3** with H atoms omitted for clarity. Thermal ellipsoids at the 50 % probability level. Selected bond lengths (Å) and angles (deg): Pt1-C1 1.941(3), Pt1-Cl1 2.3170(9), Pt1-H1 1.49(4), Pt1-N3 2.145(3); N1-C1-Pt1 113.3(2), N1-C1-N2 103.8(3), N2-C1-Pt1 142.9(3), C1-Pt1-N3 79.10(12), C1-Pt1-Cl1 173.57(11), N3-Pt1-Cl1 94.54(8).

2.4. Crystal Structure of 4.

The complex contains a C^{NHC}-bound ligand coordinated to the platinum atom, which is also coordinated to one chloride anion and one N atom. The asymmetric unit contains two molecules of benzene in addition to the Pt complex. One C_6H_6 molecule is disordered over two positions with a 0.6/0.4 ratio.

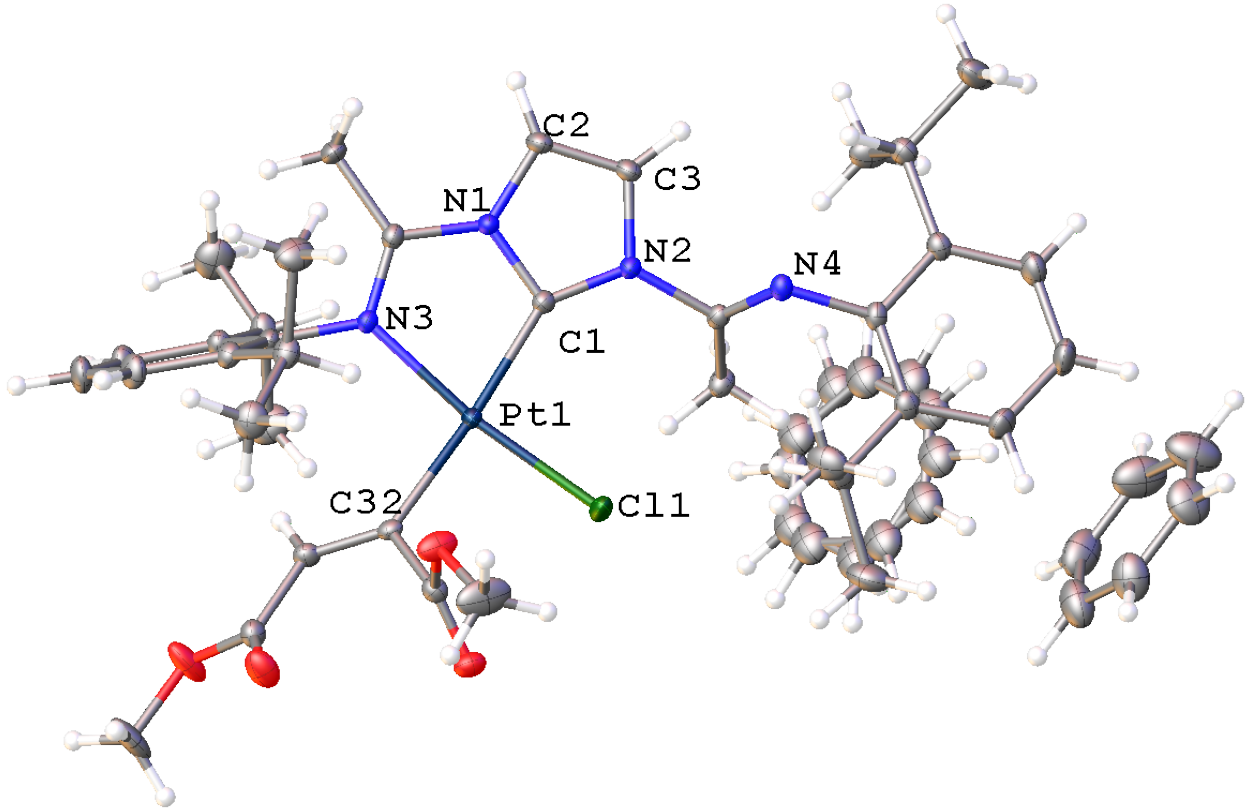

Figure S21. Structure of **4** with H atoms omitted for clarity. Thermal ellipsoids at the 50 % probability level. Selected bond lengths (Å) and angles (deg): Pt1-C1 2.0112(16), Pt1-Cl1 2.2852(5), Pt1-C32 2.0764(16), Pt1-N3 2.0469(13); N1-C1-Pt1 112.31(11), N1-C1-N2 103.56(13), N2-C1-Pt1 143.70(12), C1-Pt1-N3 78.55(6), C1-Pt1-Cl1 94.68(5), N3-Pt1-Cl1 172.25(4), N3-Pt1-C32 97.29(6), C1-Pt1-C32 174.60(6), Cl1-Pt1-C32 89.22(5).

2.5. Crystal Structure of 6.

One nitrogen atom is coordinated to the platinum atom, the hydride bound to the platinum was found (R1 = 2%).

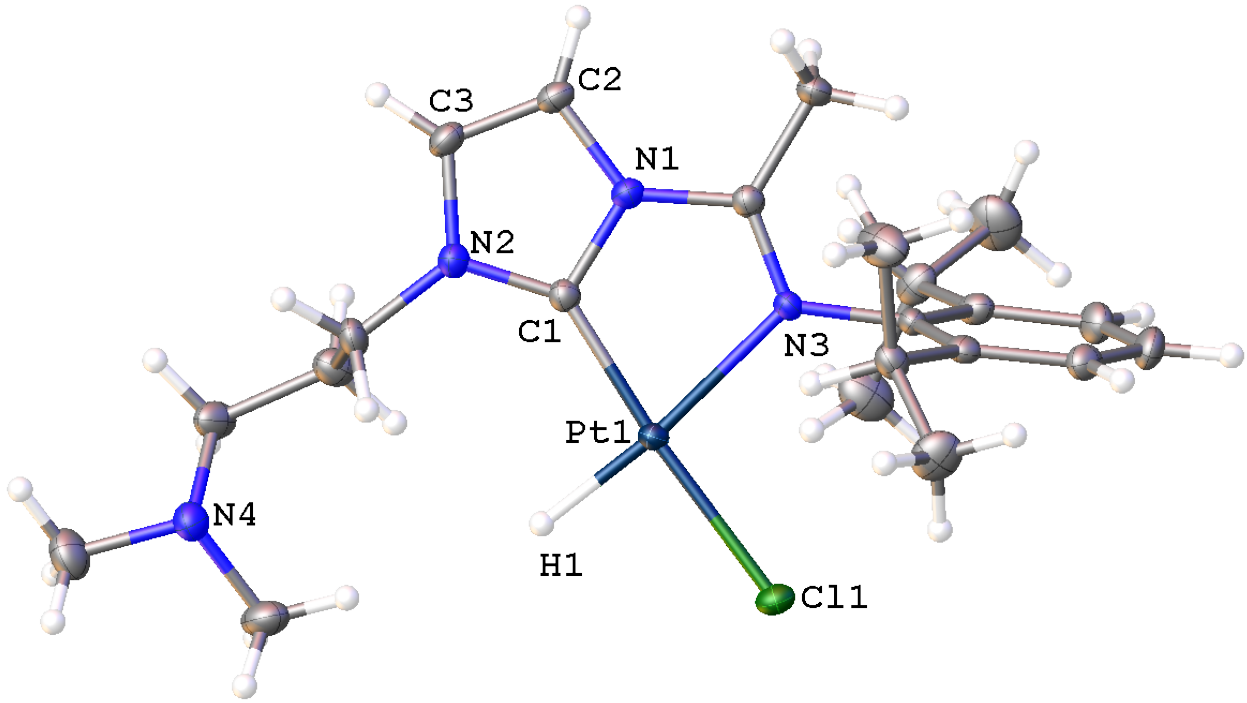

Figure S22. Structure of **6** with H atoms omitted for clarity. Thermal ellipsoids at the 50% probability level. Selected bond lengths (Å) and angles (deg): Pt1-C1 1.924(2), Pt1-Cl1 2.3502(5), Pt1-H1 1.63(3), Pt1-N3 2.1662(16); N1-C1-Pt1 115.76(15), N1-C1-N2 104.33(18), N2-C1-Pt1 139.90(16), C1-Pt1-N3 78.18(8), C1-Pt1-Cl1 175.18(6), N3-Pt1-Cl1 97.27(5).

2.6. Crystal Structure of 7.

A crystal of $C_{32}H_{51}BF_4Pt_4$, with approximate dimensions 0.050 mm x 0.090 mm x 0.100 mm, was used for the X-ray crystallographic analysis. The integration of the data using a monoclinic unit cell yielded a total of 19035 reflections to a maximum θ angle of 30.23° (0.71 Å resolution), of which 4407 were independent (average redundancy 4.319, completeness = 96.5%, R_{int} = 9.38%, R_{sig} = 9.55%) and 3319 (75.31%) were greater than $2\sigma(F^2)$. The final cell constants of *a* = 21.3229(16) Å, *b* = 12.7436(12) Å, *c* = 15.3117(14) Å, β = 132.571(3)°, *V* = 3064.1(5) $Å^3$, are based upon the refinement of the XYZ-centroids of reflections above 20 σ(I). The calculated minimum and maximum transmission coefficients (based on crystal size) are 0.5452 and 0.7456. The final anisotropic full-matrix least-squares refinement on F^2 with 171 variables converged at *R1* = 6.37%, for the observed data and wR2 = 17.11% for all data. The goodness-of-fit was 1.030. The largest peak in the final difference electron density synthesis

was 5.517 $e^-/Å^3$ and the largest hole was -4.134 $e^-/Å^3$ with an RMS deviation of 0.520 $e^-/Å^3$. On the basis of the final model, the calculated density was 2.824 g/cm^3 and *F*(000) 2384 e^-.

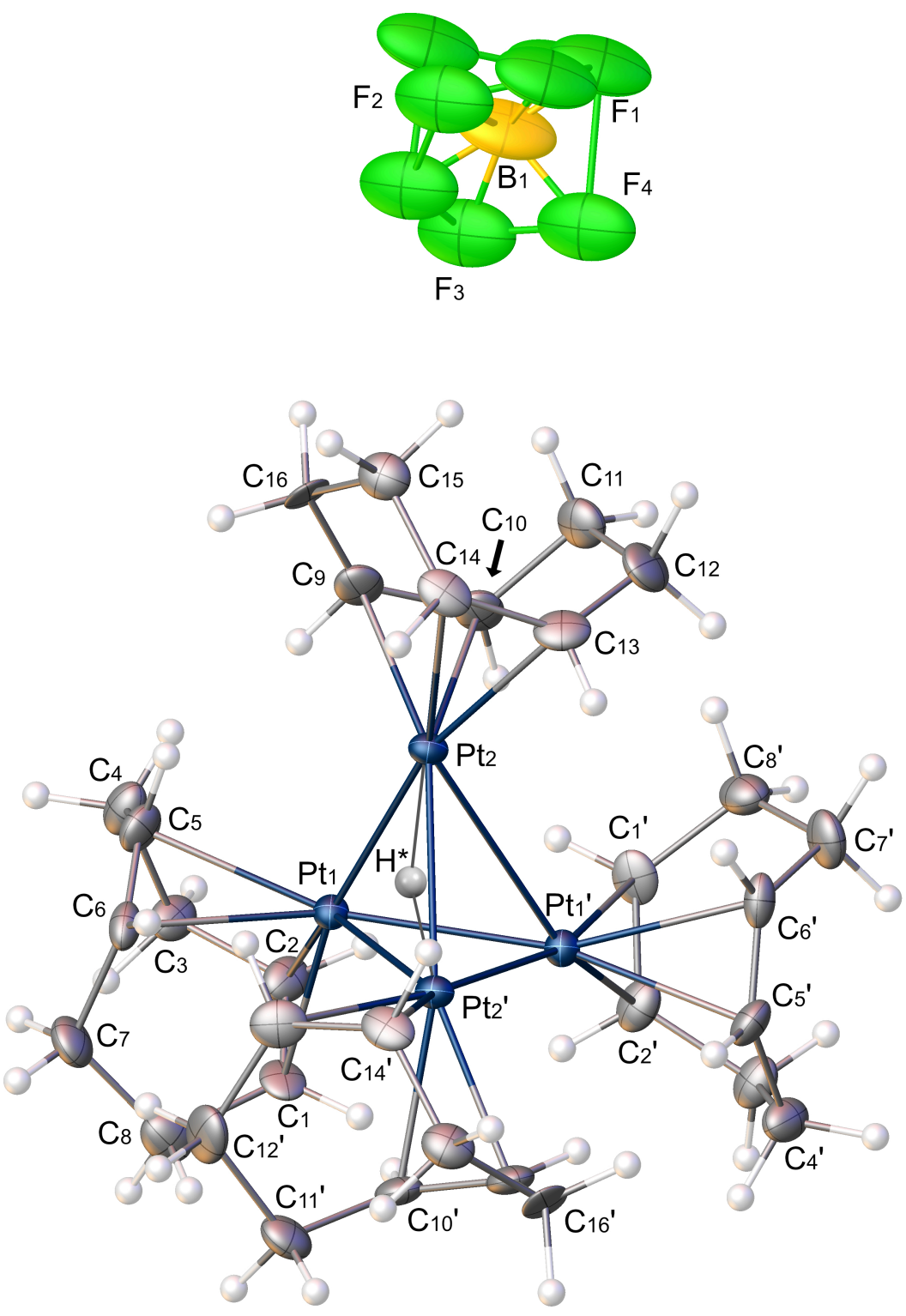

Figure S23. View of the structure of **7** with the complete labelling scheme. The anion BF_4^- is disordered over two positions. Thermal ellipsoids are shown at the 50% probability level.

Table S2. Low-Oxidation State Tetraplatinum Clusters

Entry	Formula	VEC	Structure	Pt-Pt dist. (Å)[a]		Ref
A	$[Pt_4H(PtBu^t_3)_4](BF_4)$	48		No X-ray	fluxional	6
B	$[Pt_4H_2(PtBu^t_3)_4](BF_4)_2$	48	Flattened Tetrahedron	2.609(5)–2.860(6)	fluxional	6
C	$[Pt_4(PBu_3)_3(PBu_2CMe_2CH_2\kappa^2P,C)](BF_4)$	48	Tetrahedral	No X-ray		6
D	$[Pt_4(H)_2(PBu^t_3)_4]$	50	Tetrahedral	2.667(3)–2.810(3)	fluxional	7
E	$[Pt_4(CO)_4(IPr)_3]$ (IPr = $C_3N_2H_2(C_6H_3iPr_2)_2$	54	Tetrahedral	2.685(1)–2.748(1)		8
F	$[Pt_4(\mu\text{-}CO)_2(PCy_3)_4(ReO_4)_2]$	54	Tetrahedral	2.692(1)–2.871(1)		9
G	$[Pt_4(\mu\text{-}H)_4H_3(PBu^t_3)_4](BPh_4)$*	54	Butterfly	2.636(2)–2.870(2)	fluxional	6
H	$[Pt_4(H)_8(PPr^i_2Ph)_4]$	56	Distorted Tetrahedral 4 short 2 long Pt-Pt bonds	2.848(3)–3.158(3)		7
I	$[Pt_4(\mu\text{-}CO)_3(CO)(PCy_3)_4][ReO_4]$	56	Tetrahedral	2.689(1)–2.878(1)		9
J	$Pt_4(CO)_4[\mu\text{-}\{CH_2=C(PPh_2)_2\}]_2$	56	Tetrahedral	2.593(1)–3.034(1)		10
K	$Pt_4(CO)_4(\mu\text{-dppe})_2$	56	Tetrahedral	2.5771(3)–3.0164(3)		11
L	$[Pt_4H(CO)_4[\mu\text{-}\{CH_2=C(PPh_2)_2\}]BF_4$	56	Tetrahedral	2.5992(7)–3.0470(7)		10
M	$[Pt_4H_2(CO)_4[\mu\text{-}\{CH_2=C(PPh_2)_2\}](BF_4)_2$	56	Tetrahedral	2.592(1)–3.136(1)		10
N	$[Pt_4(\mu\text{-dppm})_2(\mu\text{-}PPh_2)_2I_2]$	56	Butterfly	2.693(1)–2.874(1)		12
O	$Pt_4(\mu\text{-}CO)_5L_4$ (L = phosphines, arsines)	58	distorted tetrahedral/butterfly		Fluxional	13-15
	$[Pt_4(\mu\text{-}CO)_5(PEt_3)_4]$	58	Butterfly in the solid-state. Tetrahedral in solution	Mol 1 2.691(3)–2.766(3) (3.190(3)) Mol 2 2.704(3)–2.745(3) (3.263(3))	Fluxional	14,16
P	$[Pt_4(\mu\text{-}CO)_5(PMe_2Ph)_4]$	58	Butterfly in the solid-state. Different	2.706(2)–2.754(2) (3.543(8)	fluxional	17,18

			crystalline modifications			
Q	$[Pt_4(\mu\text{-}CO)_2(\mu\text{-}dppm)_3(\eta^1\text{-}dppm{=}O)]$	58	Butterfly	2.611(2) – 2.739(1)		19
R	$[Pt_4(\mu\text{-}H)(\mu\text{-}CO)_2(\mu\text{-}dppm)_3(PPh_3)](PF_6)$	58	Butterfly	No X-ray	fluxional	20
S	$[Pt_4(H)(\mu\text{-}CO)_2(\mu\text{-}dppm)_3(\eta^1\text{-}dppm)](PF_6)$	58	distorted tetrahedral/butterfly	2.613(1)-2.750(1) (3.082(1))		21,22
T	$[Pt_4(\mu\text{-}CO)_3(\mu\text{-}dpam)_3(\eta^1\text{-}dpam)](CF_3CO_2)_2$ (dpam = $Ph_2AsCH_2AsPh_2$)	58	Butterfly	2.604(1) - 2.713(2) (3.094(1))		23
U	$[Pt_4(\mu\text{-}CO)_3(\mu\text{-}dppm)_3(PPh_3)](PF_6)_2$	58	Butterfly	2.605(1)-2.765(1) (3.068(1))		20
V	$[Pt_4(\mu_2\text{-}H)_2(\mu_2\text{-}I)_2(\mu\text{-}dppm)_2(\mu\text{-}PPh_2)_2](O_3SCF_3)_2$	60	Rectangle	2.7728(3)-3.0058(3)		12

[a] In parentheses the distance between the wing-tip atoms in butterfly structures

* This cationic cluster reacts with ethylene at 40 °C to give $[Pt_4H(PBu^t_3)_4]^+$ which reacts with H_2 to regenerate $[Pt_4(\mu\text{-}H)_4H_3(PBu^t_3)_4]^+$.[6]

3. Computational details

All calculations were performed with GAUSSIAN 09 (version D.01).[24] package at DFT level of theory with ωB97XD functional[25] in gas phase. Carbon and Hydrogen atoms were described by Pople's 6-31+G** basis set[26] and the platinum atoms by the SDD pseudopotential and associated basis set[27]. All structures were fully optimized and the wavefunction of the minimum computed and the NBO analysis[28] performed on it. Electron Localization Function was computed on this wavefunction through TOPMOD package[29]. Non-Covalent Interactions were studied through NCIPLOT package.[30]

Table S3. Pt–Pt and Pt–H bond lengths (Å) in the different optimized clusters

	Pt–Pt	Pt–H
Exp	2.549, 2.600, 2.600, 2.778, 2.876, 2.876	
$[Pt_4(cod)_4]$	2.593, 2.593, 2.607, 2.607, 2.921, 2.921	
$[Pt_4(cod)_4]^{2+}$	2.585, 2.591, 2.591, 2.699, 2.699, 2.754	
$[Pt_4(\mu\text{-}H)(cod)_4]^+$	2.578, 2.638, 2.638, 2.851, 2.944, 2.944	1.702, 1.702

$[Pt_4(H)_2(cod)_4]$	2.618, 2.618, 2.626, 3.000, 3.343, 3.343	1.582, 1.582
$[Pt_4(H)_3(cod)_4]^+$	2.730, 2.909, 2.909, 2.919, 2.937, 2.937	1.626, 1.730, 1.915

Table S4. Electron population of the platinum shell in $[Pt_4(cod)_4]$ and $[Pt_4(\mu\text{-}H)(cod)_4]^+$

	$[Pt_4(cod)_4]$			$[Pt_4(\mu\text{-}H)(cod)_4]^+$		
	5d	6s	6p	5d	6s	6p
Pt_1	8.91	0.51	0.59	8.90	0.48	0.53
Pt_1'	8.91	0.51	0.59	8.90	0.48	0.53
Pt_2	8.91	0.51	0.59	8.99	0.47	0.55
Pt_2'	8.91	0.51	0.59	8.99	0.47	0.55

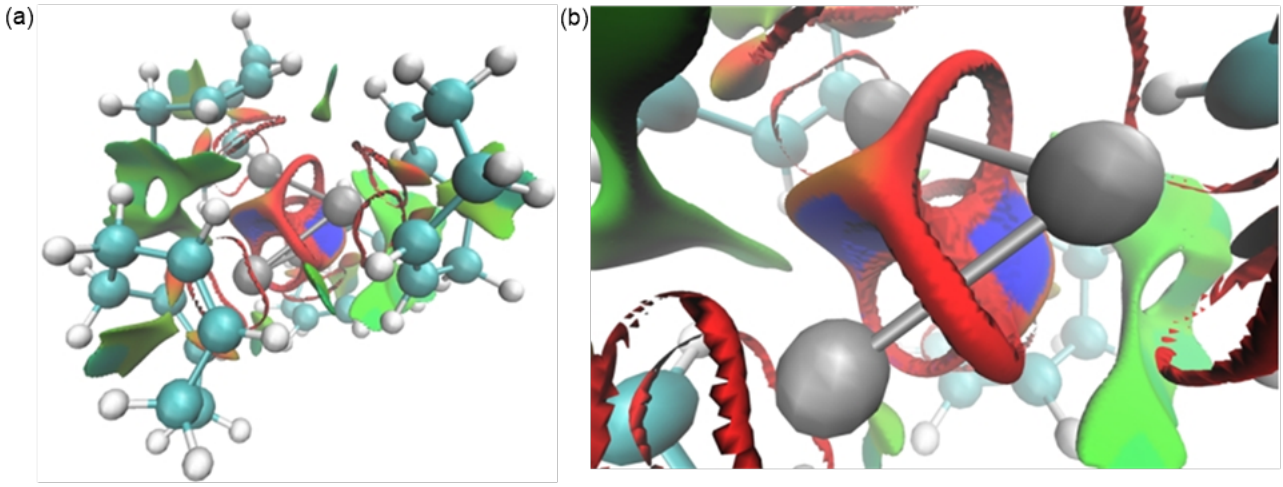

Figure S24. NCI analysis of the $[Pt_4(cod)_4]$ model complex. Areas in red correspond to steric repulsion, in green to attractive van der Waals forces, and in blue to attractive electrostatic interactions. The whole molecule (a) and a zoom of the Pt_4 core (b) are presented.

References

1. D. B. Dell'Amico, L. Labella, F. Marchetti and S. Samaritani, *J. Org. Chem.*, **2011**, *696*, 1349-1354.

2. P. Liu, M. Wesolek, A. A. Danopoulos and P. Braunstein, *Organometallics*, **2013**, *32*, 6286-6297.

3. X. Ren, C. Gourlaouen, M. Wesolek and P. Braunstein, *Angew. Chem. Int. Ed.*, **2017**, *56*, 12557-12560.

4. G. M. Sheldrick, *Acta Cryst.*, **1990**, *A46*, 467-473.

5. G. M. Sheldrick, Universität Göttingen: Göttingen Germany, **1999**.

6. R. J. Goodfellow, E. M. Hamon, J. A. K. Howard, J. L. Spencer and D. G. Turner, *J. Chem. Soc., Chem. Commun.*, **1984**, 1604-1606.

7. P. W. Frost, J. A. K. Howard, J. L. Spencer, D. G. Turner and D. Gregson, *J. Chem. Soc., Chem. Commun.*, **1981**, 1104-1106.

8. M. Bortoluzzi, C. Cesari, I. Ciabatti, C. Femoni, M. C. Iapalucci and S. Zacchini, *Inorg. Chem.*, **2017**, *56*, 6532-6544.

9. L. Hao, J. J. Vittal, R. J. Puddephatt, L. Manojlović-Muir and K. W. Muir, *J. Chem. Soc., Chem. Commun.*, **1995**, 2381-2382.

10. I. Ciabatti, C. Femoni, M. C. Iapalucci, G. Longoni and S. Zacchini, *Organometallics*, **2013**, *32*, 5180-5189.

11. C. Cesari, I. Ciabatti, C. Femoni, M. C. Iapalucci, F. Mancini and S. Zacchini, *Inorg. Chem.*, **2017**, *56*, 1655-1668.

12. W. Schuh, H. Wachtler, G. Laschober, H. Kopacka, K. Wurst and P. Peringer, *Chem. Commun.*, **2000**, 1181-1182.

13. J. Chatt and P. Chini, *J. Chem. Soc. (A)*, **1970**, 1538-1542.

14. R. F. Klevtsova, E. N. Yurchenko, L. A. Glinskaya, E. B. Burgina, N. K. Eremenko and V. V. Bakakin, *J. Struct. Chem.*, **1985**, *26*, 216-224.

15. D. G. Evans, M. F. Hallam, D. M. P. Mingos and R. W. M. Wardle, *J. Chem. Soc., Dalton Trans.*, **1987**, 1889-1895.

16. V. F. Yudanov, N. K. Eremenko, E. G. Mednikov and S. P. Gubin, *J. Struct. Chem.*, **1984**, *25*, 41-44.

17. R. G. Vranka, L. F. Dahl, P. Chini and J. Chatt, *J. Am. Chem. Soc.*, **1969**, *91*, 1574-1576.

18. A. Moor, P. S. Pregosin, L. M. Venanzi and A. J. Welch, *Inorg. Chim. Acta*, **1984**, *85*, 103-110.

19. A. A. Frew, R. H. Hill, L. Manojlovic-Muir, K. W. Muir and R. J. Puddephatt, *J. Chem. Soc., Chem. Commun.*, **1982**, 198-200.

20. B. T. Sterenberg, R. Ramachandran and R. J. Puddephatt, *J. Cluster Sci.*, **2001**, *12*, 49-59.

21.G. Douglas, L. Manojlovic-Muir, K. W. Muir, M. C. Jennings, B. R. Lloyd, M. Rashidi and R. J. Puddephatt, *J. Chem. Soc., Chem. Commun.*, **1988**, 149-150.

22. G. Douglas, L. Manojlovic-Muir, K. W. Muir, M. C. Jennings, B. R. Lloyd, M. Rashidi, G. Schoettel and R. J. Puddephatt, *Organometallics*, **1991**, *10*, 3927-3933.

23. T. Zhang, M. Drouin and P. D. Harvey, *J. Cluster Sci.*, **1998**, *9*, 165-184.

24. Gaussian 09, Revision A.02, M. J. Frisch, G. W. Trucks, H. B. Schlegel, G. E. Scuseria, M. A. Robb, J. R. Cheeseman, G. Scalmani, V. Barone, G. A. Petersson, H. Nakatsuji, X. Li, M. Caricato, A. Marenich, J. Bloino, B. G. Janesko, R. Gomperts, B. Mennucci, H. P. Hratchian, J. V. Ortiz, A. F. Izmaylov, J. L. Sonnenberg, D. Williams-Young, F. Ding, F. Lipparini, F. Egidi, J. Goings, B. Peng, A. Petrone, T. Henderson, D. Ranasinghe, V. G. Zakrzewski, J. Gao, N. Rega, G. Zheng, W. Liang, M. Hada, M. Ehara, K. Toyota, R. Fukuda, J. Hasegawa, M. Ishida, T. Nakajima, Y. Honda, O. Kitao, H. Nakai, T. Vreven, K. Throssell, J. A. Montgomery, Jr., J. E. Peralta, F. Ogliaro, M. Bearpark, J. J. Heyd, E. Brothers, K. N. Kudin, V. N. Staroverov, T. Keith, R. Kobayashi, J. Normand, K. Raghavachari, A. Rendell, J. C. Burant, S. S. Iyengar, J. Tomasi, M. Cossi, J. M. Millam, M. Klene, C. Adamo, R. Cammi, J. W. Ochterski, R. L. Martin, K. Morokuma, O. Farkas, J. B. Foresman, and D. J. Fox, Gaussian, Inc., Wallingford CT, **2016**.

25. J.-D. Chai and M. Head-Gordon, *Phys. Chem. Chem. Phys.*, **2008**, *10*, 6615-6620.

26. G. A. Petersson, A. Bennett, T. G. Tensfeldt, M. A. Al-Laham, W. A. Shirley, and J. Mantzaris, *J. Chem. Phys.*, **1988**, *89*, 2193-2218.

27. D. Andrae, U. Haeussermann, M. Dolg, H. Stoll, and H. Preuss, *Theor. Chem. Acc.*, **1990**, *77*, 123-141.

28. J. P. Foster and F. Weinhold, *J. Am. Chem. Soc.*, **1980**, *102*, 7211-7218.

29. S. Noury, X. Krokidis, F. Fuster and B. Silvi, *Comput. Chem.*, **1999**, *23*, 597–604.

30. E. R. Johnson, S. Keinan, P. Mori-Sánchez, J. Contreras-García, A. J. Cohen, and W. Yang, *J. Am. Chem. Soc.*, **2010**, *132*, 6498–6506.